

**Monoclonal Antibodies to Bovine Serum
Albumin: Affinity Purification and
Physicochemical Characterization**

by

Brian David Laffey

B.S.Ch.E., University of Iowa
(1987)

M.S.C.E.P., Massachusetts Institute of Technology
(1989)

Submitted to the Department of Chemical Engineering
in partial fulfillment of the requirements for the degree of

Master of Science in Chemical Engineering

at the

MASSACHUSETTS INSTITUTE OF TECHNOLOGY

February 1995

© Massachusetts Institute of Technology 1995. All rights reserved.

Author
Department of Chemical Engineering

February 3, 1995

Certified by ?.....

Clark K. Colton

Professor of Chemical Engineering

Thesis Supervisor

Accepted by
Science

Robert E. Cohen

Chairman, Committee for Graduate Students

FEB 17 1995

Monoclonal Antibodies to Bovine Serum Albumin: Affinity Purification and Physicochemical Characterization

by

Brian David Laffey

Submitted to the Department of Chemical Engineering
on February 3, 1995, in partial fulfillment of the
requirements for the degree of
Master of Science in Chemical Engineering

Abstract

Four monoclonal antibodies (mAb) to bovine serum albumin (BSA) were purified from mouse ascites fluid by the method of affinity chromatography. Two different affinity devices with approximately the same binding capacity for antibody were used: a column containing Sepharose CL-4B resin and an Acti-Disk GTA membrane cartridge, both of which having BSA covalently coupled to the matrix. Significant quantities (> 0.5 mg) of clones 3C2, 3C9, 1N3 and 1N16 were successfully obtained using these two devices; attempts to obtain a fifth mAb (clone 2-11) in purified form were unsuccessful. Native polyacrylamide gel electrophoresis showed that the highest purity was obtained when using the Sepharose column. Use of the Acti-Disk cartridge required an extra washing step in order to yield mAb of sufficient purity for use in later experiments.

Association constants (K_a) for each of the four mAb purified were determined by radioimmunoassay. The constants (in M^{-1}) obtained by Scatchard analysis of the data were as follows: 3C2, 5.6×10^7 ; 3C9, 1.3×10^7 ; 1N3, 1.2×10^8 ; 1N16, 4.1×10^7 . The Scatchard data for clones 3C2 and 1N16 displayed linear behavior, whereas the data for clones 3C9 and 1N3 were highly nonlinear. Values of K_a determined for 3C2 and 1N16 therefore represent intrinsic association constants, whereas those for 3C9 and 1N3 represent average affinities. Quasi-elastic light scattering (QLS) was used to investigate the sizes of complexes formed from BSA and pairs of anti-BSA mAb. With one pair (3C2 + 1N16), QLS showed an increase in the average hydrodynamic radius of the system as the concentrations of BSA and mAb increased. Size distributions of complexes formed from this pair and two other pairs (3C2 + 1N3 and 3C9 + 1N16) at a single concentration were also obtained by CONTIN analysis of QLS data. Diameters ranging from 6 to 50 nm were observed in each distribution, indicating the presence of complexes containing between one and five mAb.

Thesis Supervisor: Clark K. Colton

Title: Professor of Chemical Engineering

Acknowledgments

First, I would like to thank my advisor during this thesis, Clark Colton. His tremendous patience with me during my stay did not go unnoticed nor unappreciated. He may not realize it, but I have learned a lot from him during my time here. I am grateful to him for giving me that opportunity to learn.

I consider it a privilege to have served as a teaching assistant for Eric Anderson. His consideration and appreciation for my efforts and his respect for my opinions made me feel more like a peer than a servant. I will never forget his kindness nor his words of encouragement.

Dr. Zhiguo Su was instrumental in assisting me during the early phases of this work. He was also a friend and teacher whom I think of often, and miss to this day.

Thanks are due to John Inderdohnen of Brookhaven Instruments and Pak Yuet of this department, both of whom helped me in performing the light scattering experiments. I would also like to thank Professors Blankschtein, Hatton and Deen for allowing me time on the light scattering apparatus in their lab.

Mike Pomianek helped introduce me to a research field of which I had little prior knowledge, and taught me a great deal about experimental technique. I thank him for all his help.

David Corbin and Frank D'Ippolito were two of the first friends I made when I arrived here so many years ago. The times I spent with them were among the best times of my life. I am certain that my memories of those times will remain with me for the rest of my life.

Abdul Barakat is a man and scientist for whom I have great respect and admiration. I have never known anyone so close to my age to be as dedicated and devoted to the things that he believes are right. I am indeed lucky to call him my friend.

Sujatha Karoor is a very special person whom I have had the great fortune of knowing. She has taught me more about other people, about other cultures and about myself than anyone else ever has. I thank her for all she has done for me.

Stathis Avgoustiniatos and Leo Lue are two of the best friends I have ever known.

Stathis was always willing to listen to anything I had to say, and in times of trouble was able to offer support with a special understanding few others would have had. Leo, in many ways, has been like a second brother to me. In some ways he has been like a younger brother, because of his youthful enthusiasm and his eagerness to accept. In others, he has been like an older brother, because of his advanced knowledge and wisdom, both of which I doubt I will ever possess. I hope in some small way these two are aware of what their friendship has meant to me. I have no doubt that I am a better person for having known them.

I would also like to thank several others for their friendship and support: Alex Diaz, Thomas Kettler, Russ Kuroda, Nelson Lin (sorry for stealing the Shakespeare quote), Joy Mendoza, Ayal Naor, Costas Patrickios, Hiroshi Saito, Tim Schick; and my other labmates, Sunil Konath, Sue Lessner, Bobby Padera, and Haiyan Wu.

When people speak of the whole world living as brothers, such words carry special significance to me because of the relationship I have had with my brother Greg. With great pride and admiration I have watched him grow—albeit from a distance—into the fine young man that he is today. If it's true that younger brothers sometimes try to emulate older brothers, other times, as in our case, the opposite is equally true.

Somewhere, in some language, the name Rebecca must translate as “beacon of light,” for to those who know her, that is what my sister is. Her ability to illuminate the lives of those around her is a gift which I find more beautiful and amazing the longer I know her. She is without question the best person I have ever known.

And finally, to my mother and father. Throughout my life they have tried, with varying degrees of success, to instill in me all the qualities which make a person good and honorable. The gifts they have given—whether deserved or otherwise—I consider to be more precious than any riches the world could hold. My debt to them is truly without bound and is one that can never be repaid. I can only offer them all the thanks and love that a son can give.

Beggar that I am, I am even poor in thanks.

-William Shakespeare, *Hamlet*, Act II, Scene 1

The Well

Like a well, my thoughts intrepid,
too, run chasm deep.

Evaporate like mist upon the air.

They quench the parched soul

Who lingers there and

reaches down in hopes to

find some peace of mind.

They spring eternal as I yet

do breathe

and pour forth drenching those

who will retrieve.

My cup, it runneth o'er

today—although tomorrow

not a drop may be.

—Rebecca R. Phipps

Contents

1	Introduction and Thesis Objectives	9
1.1	Antibodies and Humoral Immunity	9
1.2	Monoclonal Antibodies	12
1.3	Bovine Serum Albumin	13
1.4	Thesis Objectives	14
2	Affinity Purification of Monoclonal Antibodies	15
2.1	Introduction	15
2.2	Materials and Methods	16
2.2.1	Materials	16
2.2.2	Methods	18
2.3	Results and Discussion	22
3	Immunologic and Physicochemical Characterization of Antigen-Monoclonal Antibody Complexes	30
3.1	Introduction	30
3.2	Materials and Methods	32
3.2.1	Materials	32
3.2.2	Methods	33
3.3	Results and Discussion	41
4	Conclusions and Recommendations for Future Work	52

List of Figures

1-1	Structure of Immunoglobulin G (IgG).	10
1-2	Formation of Antigen-Antibody Complexes.	11
2-1	Principle of Affinity Chromatography	17
2-2	GTA Coupling Chemistry.	20
2-3	Affinity Chromatography Schematic.	21
2-4	UV Absorbance Trace—Purification Using BSA-Sepharose.	24
2-5	UV Absorbance Trace—Purification Using BSA-Acti-Disk Cartridge.	25
2-6	UV Absorbance Trace—Purification Using BSA-Acti-Disk Cartridge (High Salt Wash).	25
2-7	Native PAGE Gels of Purified Protein.	27
3-1	BI-SVC Sample Cell Schematic.	36
3-2	Binding Isotherm and Scatchard Plot for mAb 3C2.	42
3-3	Binding Isotherm and Scatchard Plot for mAb 3C9.	43
3-4	Binding Isotherm and Scatchard Plot for mAb 1N3.	44
3-5	Binding Isotherm and Scatchard Plot for mAb 1N16.	45
3-6	Effect of BSA Concentration on IC Size.	48
3-7	CONTIN Distribution for BSA + 3C2 + 1N16.	49
3-8	CONTIN Distribution for BSA + 3C2 + 1N3.	50
3-9	CONTIN Distribution for BSA + 3C9 + 1N16.	50

List of Tables

2.1	Monoclonal Antibodies to BSA.	16
2.2	Average Yield of Affinity-Purified mAb.	26
3.1	mAb Association Constants.	46

Chapter 1

Introduction and Thesis

Objectives

1.1 Antibodies and Humoral Immunity

The invasion by a foreign substance into humans and many other animals often results in a response to eliminate and clear the invasive substance by the host. One such response is the production of proteins known as antibodies (Ab¹). Ab are protein molecules which bind non-covalently and specifically to the substance that caused their production (called the antigen (Ag), usually another protein or polysaccharide of viral or bacterial origin). The most prevalent type of Ab is the immunoglobulin G molecule (IgG), the general structure of which is shown in Figure 1-1.

A single IgG molecule is composed of four polypeptide chains: two identical heavy chains (M.W. ~ 50 kDa each) and two identical light chains (M.W. ~ 25 kDa each) which are linked through disulfide bridges to form the Y-shaped structure shown [38]. The two arms of IgG are referred to as the Fab regions and contain the amino acid residues responsible for Ag recognition and binding. Thus, each IgG molecule contains two identical sites which can form an association with Ag. The stem region

¹Throughout this thesis, the following abbreviations will be used: Ab, antibody; mAb, monoclonal antibody; Ag, antigen; IgG, immunoglobulin G; IC, immune complexes; and BSA, bovine serum albumin.

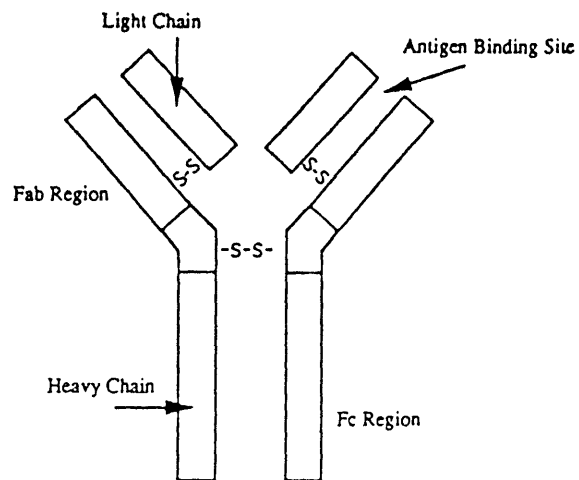


Figure 1-1: Structure of Immunoglobulin G (IgG).

of IgG is known as the Fc region and is directly involved in a number of effector functions common to many immunoglobulins, including Fc-mediated phagocytosis, antibody-dependent cell-mediated cytotoxicity, and complement activation [6].

While an Ab may have binding specificity for a particular Ag (a protein, for example), the physical association occurs only within a specific region on the Ag molecule. This physical region is known as an epitope of the Ag. Because an Ag can in principle have many epitopes within its molecular structure, a single Ag can elicit the production of many different Ab, each one having specificity for a different epitope on the same Ag. This set of all Ab produced in response to a particular Ag is known as polyclonal Ab against the Ag. Due to the multivalent nature of both polyclonal Ab and Ag, aggregates known as immune complexes (IC) can be formed when the two are combined, as shown conceptually in Figure 1-2.

When formed in the bloodstream, IC are normally cleared by the reticuloendothelial system. If these complexes are small enough and can elude clearance by such mechanisms, they can either remain in the circulation in soluble form, or can be deposited in certain tissues resulting in tissue damage and injury. In addition, they may play an immunoregulatory role in a number of diseases. Elevated levels of IC have been identified in connection with the autoimmune disorders rheumatoid arthritis,

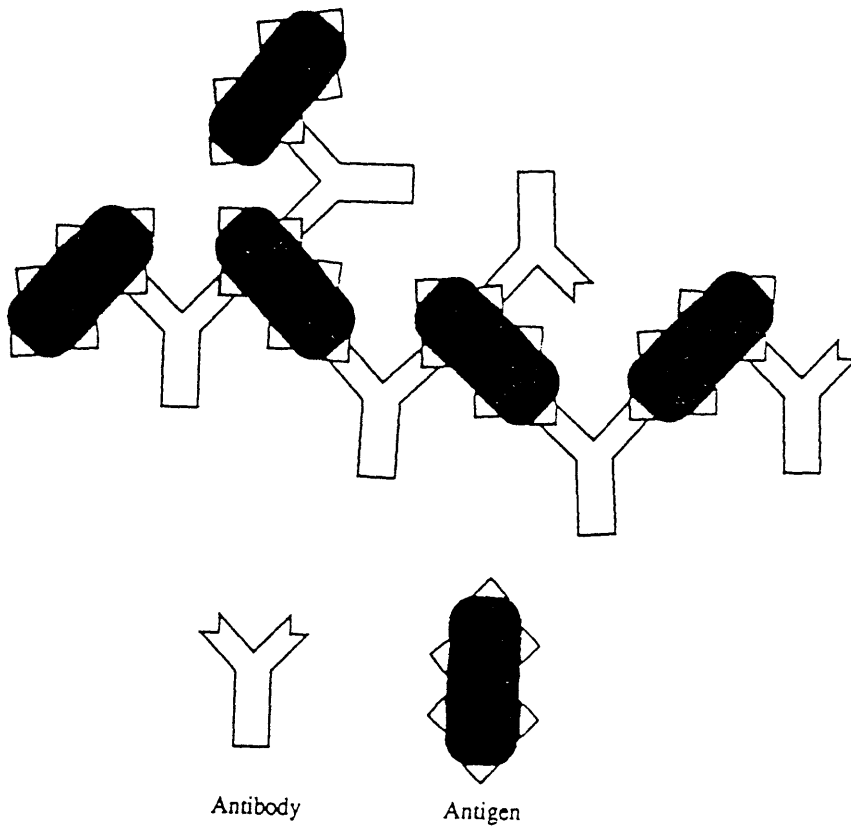


Figure 1-2: Formation of Antigen-Antibody Complexes. *Cartoon representation of divalent antibody binding to multivalent antigen to form an aggregated complex.*

systemic lupus erythmatoses, and juvenile diabetes [41, 14]; the infectious diseases viral hepatitis, bacterial endocarditis, and leprosy [41, 14]; acquired immunodeficiency syndrome (AIDS) [8]; and a variety of forms of cancer [1, 9]. A clearer understanding of the role IC play in the pathology of each of these diseases depends on knowledge of the physical chemistry of IC and of the variety of biological interactions they are involved in *in vivo*.

1.2 Monoclonal Antibodies

As mentioned above, the normal mammalian response to presentation of a single Ag is the production of polyclonal Ab, containing Ab which differ both with respect to epitope specificity and the strength of the Ab-Ag association. This is due to the fact that each individual contains an enormous number (possibly $> 10^9$ in humans) of different clones of Ab-producing lymphocytes, each of which produces an Ab unique in its precise amino acid sequence, and therefore in its Ag specificity and affinity.

A monoclonal Ab (mAb) is the product of a unique cell line known as a hybridoma cell, the development of which was first reported by Köler and Milstein in 1976 [21]. A hybridoma cell line is produced by the fusion of a mouse spleen cell (responsible for the particular Ab which is produced) to a mouse myeloma cell (allowing for unlimited cell growth and enhanced Ab secretion). Because each fused cell line obtained is derived from a single precursor B lymphocyte, the Ab produced by a particular cell line will be molecularly homogeneous. Therefore a mAb, unlike polyclonal Ab, can be characterized by a unique amino acid sequence, and can generally be characterized in terms of a specific epitope for Ag binding and a single association constant.

The development of monoclonal antibodies has led to a large number of applications involving their use. Monoclonals can be developed to a variety of protein Ag, and can be used in novel ways to probe the protein structure and function [32]. Another application involves mAb to certain cell surface proteins for use in immunocytochemistry, allowing microscopic identification of cell types [40]. Monoclonals can also aid in protein purification, where the impure protein is first used to raise mAb

to it, and then the isolated mAb is used to obtain the protein in a more purified form [16]. Development of mAb to tumor or other target Ag has also led to new diagnostic techniques and to the testing of new immunotherapies for the treatment of cancer and other diseases [11, 42].

Another interesting application involves the use of mAb to study the formation and biochemistry of Ag-Ab complexes. Relatively simple IC can be formed by mixing Ag with a small number of mAb to the Ag. These simple IC allow investigation of various aspects of IC formation and interactions utilizing a system that can be readily modeled. Previous work in this area has involved light scattering and electron microscopic studies of very simple IC in order to develop such models [30, 29, 31]. Ultimately, the complexity of the system can be increased by including greater numbers of mAb, thereby more closely mimicking the true *in vivo* situation of polyclonal Ab. The cost of this increase in complexity is the accompanying difficulty in developing models to describe the system. Recent efforts [17] have focused on this problem.

1.3 Bovine Serum Albumin

Bovine serum albumin (BSA) is a serum protein consisting of a single polypeptide chain of 582 amino acids (M.W. \sim 67 kDa), the overall structure and phylogeny of which have been studied extensively [5]. The protein consists of nine loops and can be divided into three independently-folding domains, each of which contains at least two distinct, non-cross-reacting antigenic regions [2]. Thus, the BSA molecule presents a minimum of six antigenic regions, each containing multiple epitopes, for the elicitation of Ab. Competitive binding experiments involving a panel of 64 different mAbs have identified at least 33 distinct epitopes within the BSA molecule [26].

A large number of mAb against BSA have been developed, the collection of which represents the composition of polyclonal antisera with reasonable accuracy [26]. A system consisting of BSA and mAb to BSA is therefore an attractive one for use in studying model IC.

1.4 Thesis Objectives

The objectives of this thesis were to:

1. Purify several monoclonal antibodies to bovine serum albumin using the technique of affinity chromatography.
2. Determine the equilibrium association constant for each antibody with respect to its interaction with BSA.
3. Characterize small complexes formed between pairs of antibody and BSA in solution with respect to their hydrodynamic size.

This work was motivated by the need for simple, well-characterized IC for use in protein A and complement component binding studies. Previous work had been performed in our laboratory using a set of anti-BSA mAb belonging to a non-complement-binding subclass of mouse IgG. The mAb used in this thesis belonged to mouse subclasses shown to bind and activate human complement.

Chapter 2

Affinity Purification of Monoclonal Antibodies

2.1 Introduction

In practice, mAb are generally produced by the injection of hybridoma cells into the peritoneal cavity of a mouse. Over a period of time the cells will produce the mAb and secrete their product into the ascites fluid. The fluid is then tapped several days post-injection in order to harvest the mAb. Depending on the end use, the mAb may require further purification, with different applications requiring different levels of purity. For our studies, which involved determining binding parameters and investigating sizes of Ag-mAb complexes, it was necessary to have monomeric mAb of relatively high purity.

Several techniques are commonly employed for the purification of mAb from ascites fluid. These include precipitation by ammonium sulfate [45], ion exchange chromatography [36], protein A chromatography [15], anti-Ig chromatography [18], and Ag-affinity chromatography [7]. Each of these techniques has advantages and disadvantages; some are cheap but yield mAb of low purity or specificity, while others are expensive and/or tedious but yield mAb of higher purity and specificity.

The method of affinity chromatography (see Figure 2-1) takes advantage of the fact that the protein to be purified (called the ligate, in this case the mAb) has

Clone	BSA Subdomain Specificity	IgG Subclass
3C2	3-C	IgG2b
3C9	3-C	IgG2b
1N3	1-N	IgG2a
1N16	1-N	IgG2b
2-11	2	IgG3

Table 2.1: Monoclonal Antibodies to BSA.

binding specificity for some other available protein or chemical compound (called the ligand, in this case the protein Ag). The ligand is covalently attached to some inert matrix material, and the mixture containing the ligate is contacted with this material, resulting in preferential binding of ligate to ligand. After washing any non-specifically associated species from the matrix, the ligate can then be eluted by disrupting the ligate–ligand interaction, usually by lowering the pH of the system. The result is a product of relatively high purity and specificity for the immobilized ligand. For the mAb used in our study, we chose this method of purification due to our requirement for highly pure, highly specific mAb.

2.2 Materials and Methods

2.2.1 Materials

Monoclonal Antibodies

The mAb used in this study were the generous gift of Dr. David Benjamin (University of Virginia School of Medicine, Charlottesville, VA). Five different monoclonals with binding specificity for BSA were obtained in frozen mouse ascites fluid and were stored at -70°C. Table 2.1 lists the five clones which were received, along with their corresponding IgG subclass and the subdomain on the BSA molecule (e.g., 1-N being the N-terminal region of domain 1) containing the site to which they bind.

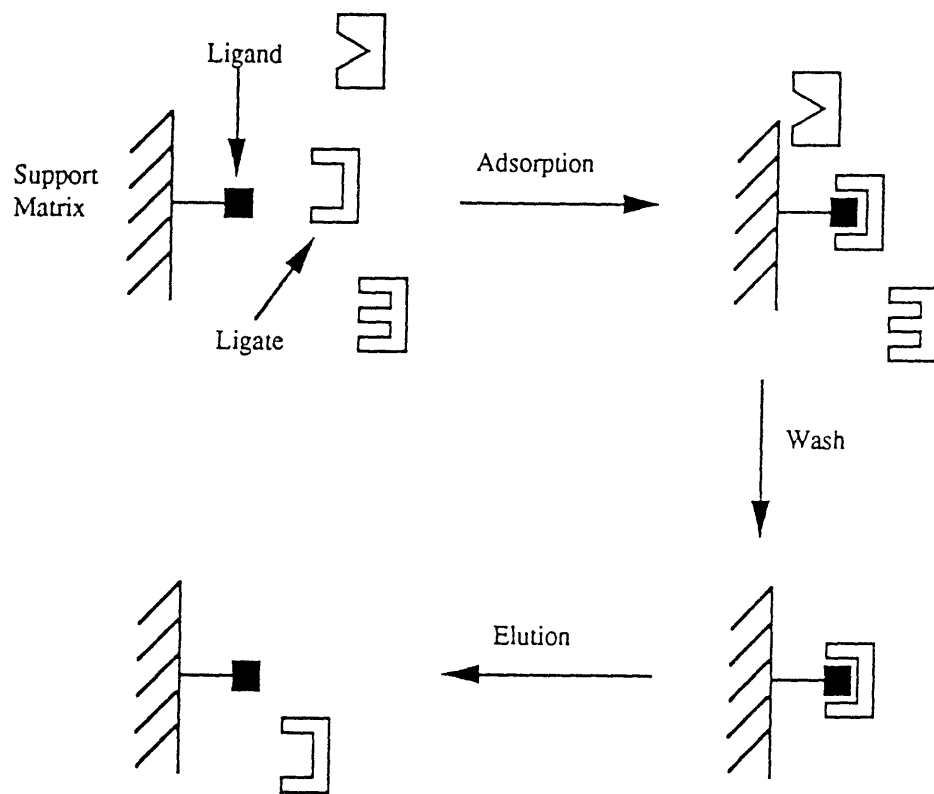


Figure 2-1: Principle of Affinity Chromatography

Affinity Supports

Two different physical support materials were used for affinity purification of mAb from ascites: Sepharose CL-4B (Pharmacia Biotech, Piscataway, NJ) and Acti-Disk GTA Cartridge (FMC BioProducts, Rockland, ME):

Sepharose CL-4B. Sepharose CL-4B is a matrix of beaded 4% agarose (wet bead diameter ranging from 45-165 μm) with the polysaccharide chains cross-linked by reaction with 2,3-dibromopropanol. The matrix is obtained in non-activated form, and must be activated chemically in order to attach the desired ligand.

Acti-Disk GTA Cartridge. The Acti-Disk GTA Cartridge consists of a microporous polymeric membrane sheet (47 mm diameter x 0.55 mm thickness) sealed in a 3 ml polypropylene housing. Glutaraldehyde groups are covalently crosslinked to the polymer matrix, resulting in a pre-chemically functionalized structure for customized ligand attachment. Amine groups of the protein to be immobilized react with the glutaraldehyde moieties within the matrix according to Schiff base chemistry, and these bonds can be stabilized by reduction with sodium borohydride.

Bovine Serum Albumin

BSA, fraction V powder, was obtained from the Sigma Chemical Co. (St. Louis, MO), and was dissolved in buffers appropriate for coupling to each material. Concentrations of BSA in solution were determined by measuring optical density at 280 nm using a model DU-50 single-beam spectrophotometer (Beckman Instruments, Somerset, NJ) and assuming an extinction coefficient for BSA of 0.66 ml/(mg-cm).

2.2.2 Methods

Ligand Immobilization

Immobilization of BSA to Sepharose. Sepharose CL-4B was activated using 1-cyano-4-dimethylamino pyridinium tetrafluoroborate (CDAP) resulting in the formation of

active cyanate ester groups ($-O-C\equiv N$) on the carbohydrate resin [22]. Approximately 25 grams of resin was first drained (Sephacrose CL-4B is packaged in 20% ethanol) on a fritted glass funnel and then washed sequentially with 100 ml of each of the following: water, ice-cold 30% acetone in water, and ice-cold 60% acetone in water. The washed Sepharose was then resuspended in 25 ml ice-cold 60% acetone, and the flask containing the suspension was placed in an ice bath mounted on an orbital shaker. Under vigorous agitation, 0.625 ml of 0.1 g/ml CDAP (Sigma) in water was then added, and the activation reaction was initiated by addition of 0.5 ml of 0.2 M triethylamine in water, 50 μ l at a time. The reaction was allowed to proceed for 2 minutes, after which time the suspension was transferred into 250 ml ice-cold washing medium (acetone:0.1 N HCl = 1:1). Prior to the coupling step, the Sepharose resin was washed on a fritted glass funnel with 1 liter of cold water, followed by 1 liter cold coupling buffer (0.1 M sodium bicarbonate, pH 8.5).

Coupling of BSA to the activated resin was performed in a similar fashion as for CNBr-activated materials [23]. Washed and activated Sepharose was first transferred to a flask containing 25 ml of 10 mg/ml BSA dissolved in the bicarbonate coupling buffer. The coupling reaction was allowed to proceed with agitation overnight at 4°C. Coupling was terminated by draining the resin on a fritted glass funnel followed by washing with 1 liter phosphate-buffered saline containing sodium azide (PBSA: 0.15 M NaCl, 0.01 M KH_2PO_4/K_2HPO_4 , 0.02% (w/v) NaN_3 , pH 7.0). The washed Sepharose was finally resuspended in PBSA and stored at 4°C. The resin with BSA covalently coupled will be referred to as BSA-Sepharose or BSA-Sepharose CL-4B.

Immobilization of BSA to Acti-Disk. The Acti-Disk GTA Cartridge is pre-activated with glutaraldehyde functional groups, and is therefore ready for coupling via Schiff base chemistry, as shown in Figure 2-2. Coupling was carried out according to the manufacturer's instructions with slight modification. The cartridge was connected to a peristaltic pumping system and flushed with deionized water at a flow rate of 6 ml/min for 10 minutes. This was followed by equilibration with Buffer A (0.5 M NaCl, 0.01 M KH_2PO_4/K_2HPO_4 , pH 7.2) for 15 minutes at a flow rate of 6 ml/min.

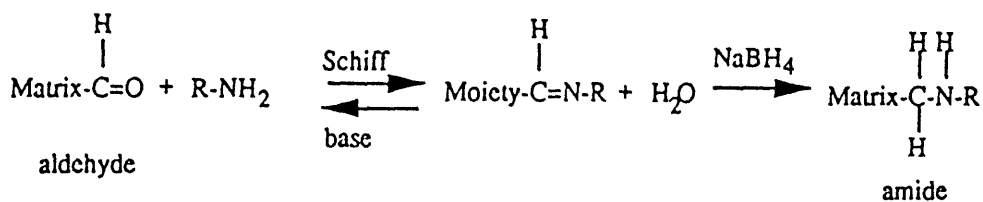


Figure 2-2: GTA Coupling Chemistry.

Coupling was performed by recirculating 40 ml of BSA in Buffer A (4 mg/ml) through the cartridge at 6 ml/min for one hour. This was followed by washing with Buffer A at 10 ml/min for 10 minutes. Blocking of residual unreacted glutaraldehyde groups was carried out by first recirculating 30 ml of 1 M Tris, pH 7.5 through the cartridge for 1 hour, followed by recirculating two separate volumes of 40 ml freshly prepared sodium borohydride in Buffer A (2 mg/ml sodium borohydride) for 1 hour each. Finally, the cartridge was flushed again with Buffer A at 10 ml/min for 10 minutes, equilibrated with PBSA, and stored at 4°C. The cartridge with BSA covalently attached will be referred to as the BSA-Acti-Disk.

Monoclonal Antibody Purification

For purifications using BSA-Sepharose, approximately 5 ml of resin was poured into a 1 cm ID glass column, and an Econo-column flow adapter (BioRad, Hercules, CA) was positioned above the settled resin. No further preparation was necessary when using the BSA-Acti-Disk cartridge. In either case, the device (column or cartridge) was installed into the chromatography system schematized in Figure 2-3. The system consisted of either a Cole-Parmer Masterflex (Niles, IL) or an ISCO Tris (Lincoln, NE) peristaltic pump, the affinity device, an ISCO UA-5 UV detector, and a Pharmacia Frac-100 fraction collector, all connected in series by Tygon tubing.

For each mAb purified using BSA-Sepharose, 600 μl of the corresponding thawed ascites fluid was diluted into 2 ml PBSA and mixed well; for purifications using the BSA-Acti-Disk, the corresponding volumes were 200 μl of ascites and 2 ml PBSA. The resulting diluted ascites was filtered twice through Millex GV 0.22 μm syringe

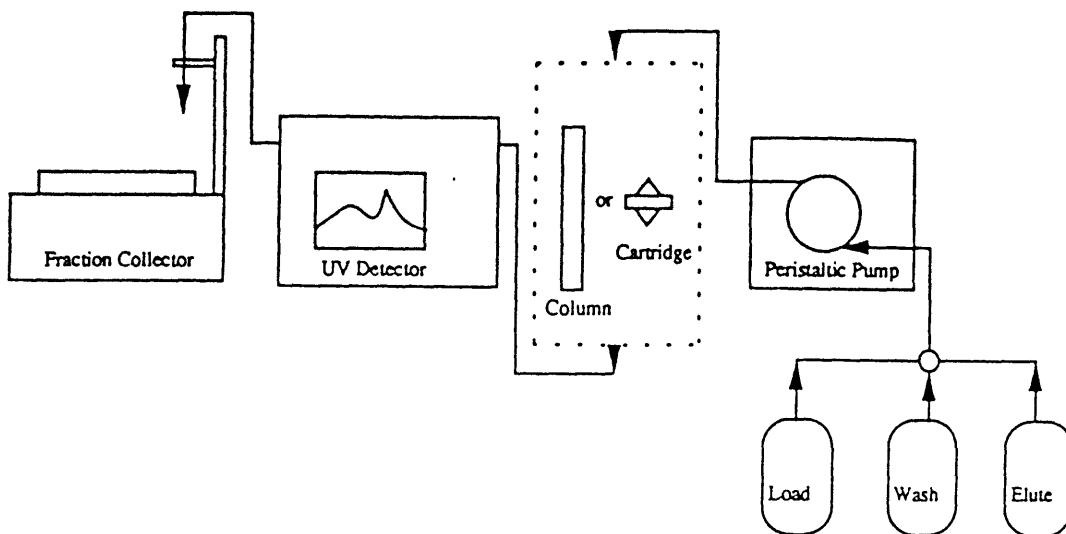


Figure 2-3: Affinity Chromatography Schematic.

filters (Millipore, Bedford, MA) prior to loading. For purifications involving the BSA-Sepharose column, a flow rate of 2.2 ml/min during loading was maintained; for those involving the BSA-Acti-Disk, a higher flow rate of 5 ml/min was used. Loading was performed either in single pass fashion, or by recirculating the diluted ascites through the device for 30 minutes. Non-specifically bound proteins were then removed by washing the column with PBSA until the UV absorbance at 280 nm reached the baseline value.

Elution of mAb was accomplished by application of a low pH glycine buffer to the column or cartridge. For runs performed using BSA-Sepharose, 0.1 M glycine/HCl, pH 2.5, was used to elute bound mAb; for those performed using the BSA-Acti-Disk cartridge, 0.1 M glycine in 2% (v/v) acetic acid, pH 3.2, was used. Later runs involving the Acti-Disk cartridge also included a “pre”-elution step, where a high salt buffer (1 M NaCl, 0.01 M KH₂PO₄/K₂HPO₄, pH 7.0) was used to remove any non-specifically adsorbed proteins from the cartridge. Protein-containing fractions collected during the low pH elution were pooled and immediately placed into Spectra/Por 7 dialysis tubing having a nominal molecular weight cutoff of 25 kDa (Spectrum, Houston,

TX). The eluted protein was dialyzed extensively against PBSA at 4°C, and concentrated using Centriprep-30 centrifugal concentrators (Amicon, Beverly, MA) in an IEC Model PR-6 swinging bucket centrifuge. Concentrations were determined by measuring the optical density at 280 nm and assuming an extinction coefficient of 1.4 ml/(mg-cm) for IgG.

Native Polyacrylamide Gel Electrophoresis (Native PAGE)

Gel electrophoresis of purified mAb was performed using a Pharmacia PhastSystem electrophoresis unit. Proteins were separated under non-denaturing, non-reducing conditions by means of gradient gels [10]. In gradient gels, the nominal pore size within the gel decreases continuously throughout; thus, under the same electric field, proteins can be separated on the basis of hydrodynamic size due to hindrance effects.

Samples of 1 μ l were applied to Pharmacia PhastGel Gradient 8-25 gels, and were separated according to the standard program provided by Pharmacia. Two lanes of Pharmacia Native PAGE High Molecular Weight Standards (containing 1 mg/ml of each of the following: albumin, M.W. 67 kDa; lactate dehydrogenase, M.W. 140 kDa; catalase, M.W. 232 kDa; ferritin, M.W. 440 kDa; and thyroglobulin, M.W. 669 kDa) were included on each gel to determine relative mobilities of sample proteins. Protein bands were visualized by coomassie blue staining (PhastGel Blue R, Pharmacia).

2.3 Results and Discussion

The amount of BSA covalently coupled to the Sepharose resin was determined by mass balance to be 3.5 mg/ml of gel, or 87.5 mg BSA total. Based on the quantities of reagents used for activation, an estimated maximum coupling capacity of 5 μ mol of ligand per ml resin has been reported using CDAP activation chemistry [22]. For BSA (M.W. \sim 67 kDa) this corresponds to a maximum coupling capacity of 334 mg/ml of gel. It would appear, then, that the coupling achieved in this study was far less than the maximum possible. This maximum capacity, however, is based on the approximate total number of active cyanate ester groups ($-\text{O}-\text{C}\equiv\text{N}$) which are

formed upon reaction of CDAP with the carbohydrate resin. Due to the porous nature of Sepharose, we would expect that many of these ester groups may be situated in regions which are inaccessible to the large BSA macromolecule. In addition, many active groups are likely to be in close proximity to one another. In such a case, an equimolar attachment of BSA molecules to these neighboring cyanate ester groups would be sterically hindered. Therefore, the amount of BSA immobilized in this study seems reasonable, and is well within the range of capacities quoted for a number of commercially-prepared affinity resins.

The amount of BSA attached to the Acti-Disk membrane was determined by mass balance to be 19.4 mg. This value is compared to an approximate maximum coupling capacity of 25–30 mg according to FMC product literature. Thus, between 65 and 78% of the maximum capacity was achieved. This failure to achieve maximum capacity was most likely the result of improper flow distribution across the membrane surface during the coupling procedure. During some steps, fluid channeling and occasional bubbles were observed within the translucent plastic housing. It is likely that portions of the membrane surface were not exposed to the BSA ligand, resulting in incomplete utilization of the GTA groups.

A total of 39 purifications of mAb were performed on ascites samples of the five clones listed in Table 2.1. Seven purifications were performed using the BSA-Acti-Disk cartridge without the high salt wash step, 22 were performed using the cartridge with the high salt wash step, and 10 were performed using the BSA-Sepharose column. The addition of the high salt wash when using the Acti-Disk cartridge was prompted by the low level of mAb purity obtained without such a step (see below and Figure 2-7).

UV absorbance data as obtained from the ISCO-UA5 detector for three of the purifications are presented in Figures 2-4 through 2-6. Several features can be seen in the figures. In each, the breakthrough of non-bound protein is marked by a large initial absorbance peak occurring a few minutes following the introduction of ascites onto the column or cartridge. This absorbance then decays in an oscillatory fashion as the ascites is recycled through the particular device, indicating that more protein is binding to the device. In the case of BSA-Sepharose, this oscillation in absorbance

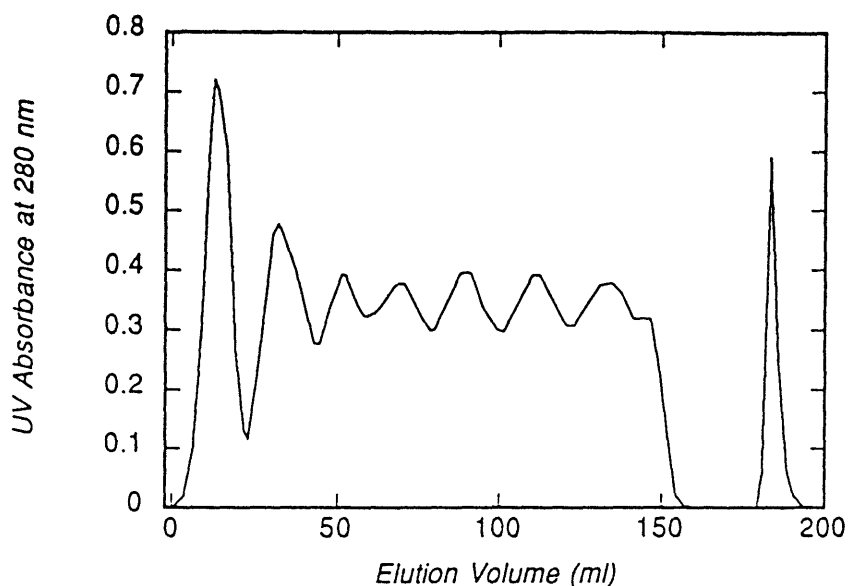


Figure 2-4: UV Absorbance Trace. *UV absorbance at 280 nm vs. elution volume for mAb 3C2 purified on BSA-Sepharose, with recycle.*

does not appear to fall after the first or second oscillation, and appears significantly more erratic than in the case of the BSA-Acti-Disk. In all three figures the absorbance fails to return to the baseline value during this recycle period, indicating that unbound protein remains in solution. The UV absorbance then quickly returns to baseline upon introduction of the PBSA wash. Finally, a sharp peak is observed corresponding to protein eluted by application of the low pH glycine buffer. In the case of Figure 2-6, there are two elution peaks: the first corresponding to weakly-associated protein eluted during the high salt buffer wash, and the second corresponding to strongly-associated protein (mAb) eluted by the glycine buffer.

The amount of protein obtained from each purification was determined, and the average yield values for each mAb/method combination are listed in Table 2.2. The numbers in parentheses correspond to the number of purifications of each mAb using each particular method. In general, the yield of each mAb decreased in the order 3C2 > 1N16 > 3C9 > 1N3 > 2-11. The yield of mAb 2-11 was extremely low (negligible when using the high salt wash/BSA-Acti-Disk); thus, no further efforts to purify this mAb were made.

The maximum binding capacity of the two affinity devices can be estimated by

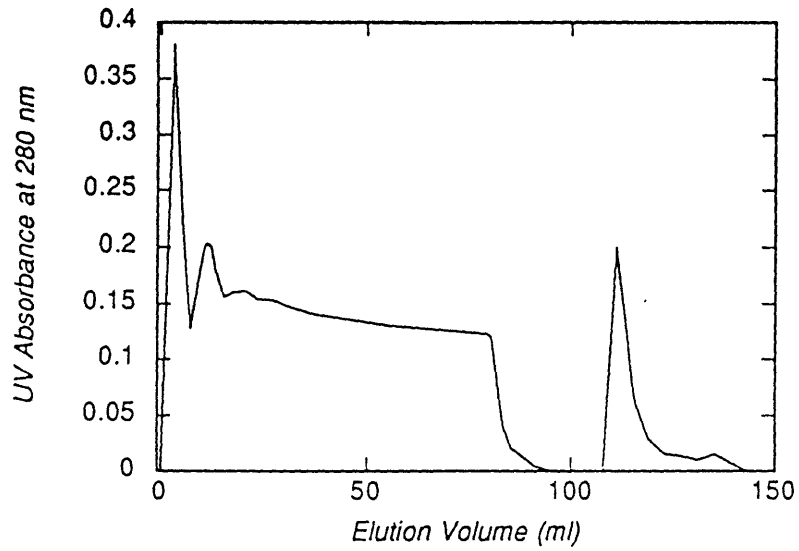


Figure 2-5: UV Absorbance Trace. *UV absorbance at 280 nm vs. elution volume for mAb 3C2 purified on BSA-Acti-Disk cartridge, with recycle. High salt wash step was not performed.*

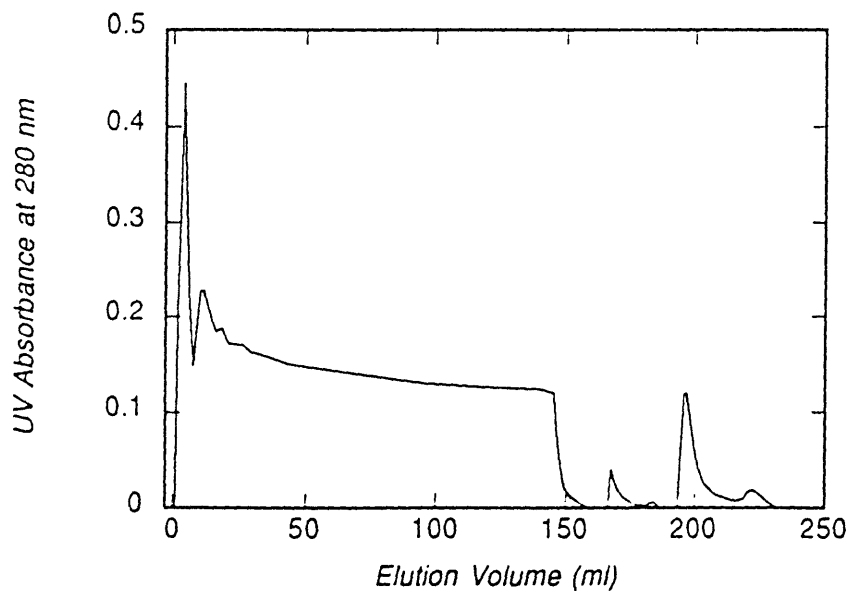


Figure 2-6: UV Absorbance Trace. *UV absorbance at 280 nm vs. elution volume for mAb 3C2 purified on BSA-Acti-Disk cartridge, with recycle. High salt wash was performed prior to elution of mAb.*

mAb	Average Yield (mg) BSA-Acti-Disk, No Wash	Average Yield (mg) BSA-Acti-Disk, High Salt Wash	Average Yield (mg) BSA-Sepharose
3C2	1.35 (2)	0.96 (4)	3.30 (5)
3C9	0.85 (1)	0.66 (5)	— (0)
1N3	0.78 (2)	0.55 (6)	— (0)
1N16	1.09 (1)	0.76 (4)	1.50 (5)
2-11	0.64 (1)	0.01 (3)	— (0)

Table 2.2: Average Yield of Affinity-Purified mAb. *mAb were purified from 0.2 ml ascites (BSA-Acti-Disk) or 0.6 ml ascites (BSA-Sepharose) as described in Section 2.2.2. Number in parentheses indicates number of purifications performed with that method.*

assuming that every BSA molecule immobilized is immunoreactive for each mAb. This assumes that each BSA molecule is immobilized such that every epitope is exposed and displays its native conformation. In such a case, the estimated maximum mAb-binding capacities would be 40.1 mg and 44.5 mg for a 5 ml column of BSA-Sepharose and the BSA-Acti-Disk cartridge, respectively. The calculated yields listed in Table 2.2 would suggest that the saturation capacity of these materials was not reached under the conditions used in this study. It is interesting to note the effects of increasing the ascites load by a factor of three using the BSA-Sepharose column versus the BSA-Acti-Disk. The average yield of mAb 3C2 obtained at this higher load increased by over a factor of three, whereas the average yield of 1N16 increased by only a factor of two. Thus, it would appear that BSA-Sepharose was slightly more efficient than the BSA-Acti-Disk for the purification of mAb 3C2 (5.5 versus 4.8 mg/ml ascites), whereas the reverse was true for the purification of mAb 1N16 (2.5 versus 3.8 mg/ml).

The eluted and dialyzed protein obtained by these three methods was analyzed by native PAGE in order to determine the electrophoretic nature and homogeneity of the product. Figure 2-7 shows three such native PAGE gels: one each for protein eluted from the BSA-Acti-Disk both with and without the high salt wash step, and one for protein eluted from BSA-Sepharose. In general, the intensities of the bands corresponding to mAb are consistent with yield measurements: intensities decrease in the order 3C2 > 1N16 > 3C9 > 1N3 > 2-11. Also evident is the difference in the

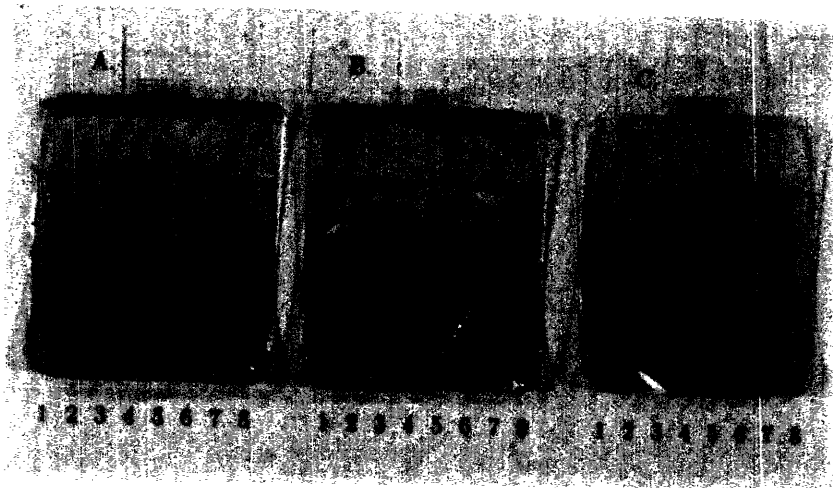


Figure 2-7: Native PAGE Gels. *A. Protein purified using BSA-Acti-Disk (without high salt wash): lane 1, MW Standards; lanes 2 and 4, 1N3; lane 3, 1N16; lane 5, 3C9; lane 6, 2-11; lane 7, 3C2; lane 8, MW Standards. B. Protein purified using BSA-Acti-Disk (with high salt wash): lane 3, MW Standards; lane 4, 1N16; lane 5, 3C9; lane 6, 3C2; lane 7, 2-11; lane 8, MW Standards. C. Protein purified using BSA-Sepharose: lane 1, MW Standards; lanes 2-5, empty; lane 6, 1N16; lanes 7, 3C2; lane 8, MW Standards. In all gels, MW increases from bottom to top.*

apparent purity using each method: the purity increases in the order BSA-Acti-Disk (no wash) < BSA-Acti-Disk (wash) < BSA-Sepharose.

As seen in Figure 2-7.A, the homogeneity of the protein obtained using the BSA-Acti-Disk without the additional wash step was especially poor, with numerous protein bands of both higher and lower molecular weight visible. This may have been due to a high degree of non-specific adsorption of other ascites proteins to the Acti-Disk membrane. In addition, the likelihood of there existing residual non-reduced glutaraldehyde groups may have contributed to this problem. As mentioned earlier, an estimated 22 to 35% of the glutaraldehyde groups available for BSA ligand attachment were not utilized during the coupling procedure. The sodium borohydride reduction step following coupling should have resulted in the inactivation of such unreacted glutaraldehyde moieties; however, the completion of this reduction step was determined visually, with the membrane color turning from reddish-brown to yellow to indicate reduction. Although the entire membrane surface did exhibit this color change, the

final yellow color was not entirely homogeneous, suggesting that small areas of the membrane may not have been exposed to chemical reduction. Any glutaraldehyde groups in such areas would have remained active and capable of binding other ascites proteins.

Because of the poor purity obtained using the BSA-Acti-Disk initially, the high salt wash step was added as a means of removing these contaminating proteins. This modification worked quite well, as evidenced by the near complete disappearance of contaminating bands in Figure 2-7.B. The few remaining faint bands correspond to low levels of proteins which could be removed further using size exclusion methods. Finally, protein obtained using BSA-Sepharose appeared to be nearly perfectly homogeneous, as seen in Figure 2-7.C, suggesting the only protein interactions which occurred using this material were those between the mAb and the BSA ligand. This result is consistent with Pharmacia's claim that the Sepharose matrix displays negligible non-specific adsorption of proteins. The mAb purified using this material were therefore judged to be of sufficient homogeneity for use in subsequent experiments.

A comment regarding the observed electrophoretic mobilities of these mAb deserves mention. For each mAb the major band showed a relative mobility slightly less than that for catalase, thus implying a corresponding molecular weight slightly greater than 230 kDa. This is inconsistent with the expected molecular weight of IgG (approximately 153 kDa), and would seem to suggest that these bands represented mAb which had formed dimers or perhaps even larger oligomers. The diversity in amino acid sequence among different mAb, however, results in corresponding differences in electric charge, and thus in their electrophoretic behavior (as seen in Figure 2-7, where bands corresponding to different mAb appear in slightly different locations on the gel). In addition, the non-globular nature of IgG may result in anomalous migration through the porous gel. A measurement of the size of one mAb (1N16) using an independent light scattering technique (QLS) suggested that its size corresponded to that of monomeric IgG. We concluded, therefore, that the major bands observed in the Native PAGE gels represented monomeric mAb, rather than oligimers of higher molecular weight.

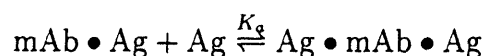
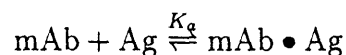
Thus, either of the two methods studied (use of BSA-Sepharose or BSA-Acti-Disk) appeared to be satisfactory for the purification of anti-BSA mAb from mouse ascites fluid, provided that an extra wash step is included when using the membrane cartridge. While it is a slightly quicker and somewhat less cumbersome technique, use of the BSA-Acti-Disk resulted in slightly lower product purity, thus requiring an additional chromatography step to obtain pure monomeric mAb.

Chapter 3

Immunologic and Physicochemical Characterization of Antigen-Monoclonal Antibody Complexes

3.1 Introduction

When a mixture of a single, non-crossreactive mAb and its univalent Ag are prepared, complexes containing the mAb and either one or two Ag molecules are formed. Assuming there are no cooperativity effects involved, this equilibrium binding between mAb and Ag can be characterized by a single intrinsic association (or affinity) constant, K_a :



A number of techniques for experimentally determining affinity constants between mAb and their Ag have been published, among them equilibrium dialysis [13], solid-

phase radioimmunoassays [25] or enzyme-linked immunosorbent assays [19], and ellipsometry measurements [33]. Equilibrium dialysis is generally not well suited for studying mAb which bind to large proteins, and several of the other techniques involve immobilizing either Ag or mAb to a solid surface, yielding results which may not represent association in solution. For our investigation we chose a radioimmunoassay technique developed and used previously in our laboratory [28, 29]. The technique was based on precipitation of mAb which had first been allowed to associate with soluble, radiolabelled Ag. The constant thus obtained should be more representative of the affinity constant in solution.

When mixtures of Ag and multiple mAb to that Ag are prepared, a distribution of IC varying in size are formed. This system of Ag, mAb and heterogeneous IC is in dynamic equilibrium; the equilibria is dependent on the concentrations of all species present and the intrinsic affinities of the mAb involved. As size is an important parameter in determining the biological properties of IC *in vivo* [27], methods to study the size distributions of IC in solution have been highly sought. Some of these methods have in the past included gel permeation chromatography [20] and sucrose density gradient ultracentrifugation [39]. In both of these, significant dilution of the system occurs, perturbing the equilibria and thus the distribution of IC in solution.

Quasi-elastic laser light scattering (QLS) offers a non-invasive technique for examining the size distribution of IC *in situ*. In QLS, a laser beam is focused on the sample of interest and the light scattered by the proteins in solution is collected at some angle from the incident beam. The intensity of this scattered light fluctuates in a time-dependent manner due to the Brownian motion of the molecules in solution; these fluctuations can in turn be analyzed in order to yield information concerning the size of the scattering species [3]. Because of the non-invasive nature of this technique, problems such as dilution are avoided.

In these studies, simple IC were constructed by mixing BSA as the protein Ag with pairs of anti-BSA mAb. Within each pair studied, each mAb bound to a different, univalent site on the BSA molecule. Under these conditions, only linear and cyclical IC can be formed. Such a system was previously shown to exhibit many in-

interesting features characteristic of naturally-occurring IC, and yet was simple enough for accurate models to be developed [29]

3.2 Materials and Methods

3.2.1 Materials

Monoclonal Antibodies

The mAb used in these experiments were those which were successfully purified in significant quantities by affinity chromatography, described in Chapter 2. In most cases, further purification using gel filtration was necessary in order to isolate samples of antibody which were essentially free of oligimers and other trace contaminants. Gel filtration was performed using a Superose 6 HR 10/30 column connected to a Fast Protein Liquid Chromatography (FPLC) system (Pharmacia Biotech) with PBSA as the running buffer. Fractions corresponding to monomeric antibody were collected and concentrated using Amicon Centricon-30 centrifugal concentrators on a Clay-Adams Sero-Fuge (Becton Dickinson, Parsippany, NJ). Concentrations were determined by measuring optical density at 280 nm and assuming an extinction coefficient for IgG of 1.4 ml/(mg-cm). Antibodies were stored at 4°C in stock solutions ranging in concentration between 1 and 2 mg/ml.

Bovine Serum Albumin

BSA, monomer standard powder, was obtained from ICN Biomedicals (Costa Mesa, CA), and was dissolved in PBSA to approximately 2 mg/ml. Further purification was necessary to isolate monomeric BSA free of oligimers. As with the monoclonal antibodies, gel filtration was performed using a Superose 6 HR 10/30 column connected to a Pharmacia FPLC system. Fractions which corresponded to monomeric BSA were collected and concentrated using Amicon Centricon-10 concentrators on a Clay-Adams Serofuge. Concentrations were determined by measuring optical density at 280 nm and assuming an extinction coefficient for BSA of 0.66 ml/(mg-cm). Stock

solutions of monomeric BSA in PBSA (between 1 and 3 mg/ml) were stored at 4°C.

3.2.2 Methods

Radiolabelled BSA Binding Experiments

BSA was labelled with I^{125} by the use of IODOBEAD reagent (Pierce Chemical, Rockford, IL). The BSA used for labelling was prepared as described above and diluted in PBSA on the day of labelling (300 μ g into 500 μ l in 3 ml polyethylene tubes). To this was added 500 μ Ci of NaI^{125} (NEN Research Products, Boston, MA), followed by two pre-rinsed IODOBEADs. The iodination reaction was allowed to proceed for 15 minutes, and was stopped by removing the mixture from the polyethelene tube. The beads were quickly washed twice with one ml of PBSA to maximize protein recovery, and the washes were added to the removed BSA. The recovered protein was then loaded onto a small BioRad 10DG desalting column in order to remove non-incorporated label from the protein. Fractions which contained labelled protein were collected and concentrated using Centricon-10 microconcentrators on a Clay-Adams Serofuge. Activity measurements (in counts per minute, or CPM) were made using an Auto-Gamma 500 gamma-counter (Packard Instrument Co., Downer's Grove, IL). To ensure that most of the activity present corresponded to labelled protein, 10% trichloroacetic acid was added to precipitate BSA- I^{125} , and the activity of precipitate and supernatant were measured. Specific activities of the labelled BSA were determined prior to each binding experiment by counting 100 μ l aliquots of solutions of known BSA- I^{125} concentration.

The method used for the determination of binding constants was modified slightly from one published previously [29]. For each experimental assay, an appropriate volume of diluent was first added to 250 μ l polyethylene microcentrifuge tubes. The diluent used (referred to as PBSA-TT) was PBSA which contained 0.5 mg/ml porcine thyroglobulin (Sigma Chemical Co.) to prevent non-specific binding, and 0.05% (v/v) Tween 20 (Sigma Chemical Co.) to prevent adsorption to surfaces. To each tube was added the mAb being studied at a total concentration of 2×10^{-8} M, followed by an

amount of radiolabelled BSA varying between 3×10^{-9} and 3×10^{-7} M. Volumes of each reactant were chosen such that the total volume (diluent plus mAb and BSA- I^{125}) was $150 \mu\text{l}$. In order to precipitate all the antibody in each tube, $50 \mu\text{l}$ of a slurry (25% (v/v) in PBSA-TT) of agarose beads to which anti-mouse IgG had been coupled (Sigma Chemical Co.) was added. The tubes were quickly mixed using a vortex mixer, and were rotated end-over-end at room temperature for two to three hours to reach equilibrium. The tubes were then centrifuged for five minutes in a Microfuge B (Beckman Instruments) and $100 \mu\text{l}$ of supernatant was removed and transferred to a second microcentrifuge tube. The activity in both precipitate and supernatant tubes was counted, and concentrations of BSA both bound to antibody and free in solution were determined as follows:

$$[BSA]_{bound} = \frac{CPM_{precipitate} - CPM_{supernatant}}{V_{total}(SA)} \quad (3.1)$$

$$[BSA]_{free} = \frac{CPM_{supernatant}}{V_{supernatant}(SA)} \quad (3.2)$$

where $CPM_{precipitate}$ and $CPM_{supernatant}$ are the measured counts per minute of the precipitate and supernatant tubes, respectively; V_{total} and $V_{supernatant}$ are 200 and $100 \mu\text{l}$, respectively; and (SA) is the measured specific activity of the labelled BSA in CPM/mole. Triplicate assays were performed at each BSA- I^{125} concentration.

The assay was developed such that all the antibody present will be precipitated by addition of anti-IgG beads. Under these conditions, the association constant, K_a , can be determined by the familiar Scatchard equation:

$$\frac{[BSA]_{bound}}{[BSA]_{free}} = bK_a[mAb]_{total} - K_a[BSA]_{bound} \quad (3.3)$$

where b corresponds to the valence of the antibody (in this case, $b = 2$). Plotting the ratio of bound to free concentrations of BSA versus the bound concentration should result in a straight line whose negative slope corresponds to the association constant.

Quasi-Elastic Laser Light Scattering

Experimental. All measurements were taken using a Brookhaven Instruments (Holtsville, NY) light scattering system consisting of a Lexel Model 95 argon ion laser, a Thorn EMI model B2FBK/RF1 electron tube, and a Brookhaven BI-9000AT autocorrelator. The laser was operated in the power-control mode at a maximum power of 300 mW and a wavelength of 514 nm. Scattered light was detected by the electron tube at an angle of 90° from the incident beam. The sample chamber was maintained at a temperature of $20.0 \pm 0.2^\circ\text{C}$ by means of a Neslab RTE-1000 water bath (Neslab, Portsmouth, NH). The autocorrelator delay times were adjusted such that the autocorrelation function displayed a smooth exponential decay, and the total time for a single measurement was generally set at 120 seconds.

Two types of sample cells were used: the BI-SVC (Small Volume Cell, Brookhaven Instruments) and 10x75 mm borosilicate glass culture tubes (VWR Scientific, San Francisco, CA). The BI-SVC consisted of a brass holder, a white cone-shaped teflon sleeve, and the actual sample cell. The sample cell consisted of two pieces: a 10 mm OD, 8 mm ID borosilicate glass cell of height 70 mm, and a black teflon insert machined to fit snugly into the glass cell. The black teflon insert had a small hole bored along the centerline of the insert, from the top down to a point approximately 8 mm from the bottom. Here a 1.5 mm wide slit was notched into the side, allowing a very small volume within the insert to be illuminated by the laser (see Figure 3-1).

Measurements were taken on samples which had first been filtered twice through Millipore HV 0.45 μm syringe tip filters in order to remove dust and any large aggregates. When using the BI-SVC, the black teflon insert was lowered into the glass cell, and approximately 50 μl of sample was injected via syringe into the hole bored within the insert, taking care not to overfill the volume formed by the notch. The glass cell was then covered, inserted into the white teflon sleeve, and the sleeve was placed in the brass holder positioned in the QLS sample chamber. The position of the cell in the sleeve was raised or lowered so that the laser beam passed directly through the notch in the insert. When using 10x75 mm glass culture tubes, approximately 300

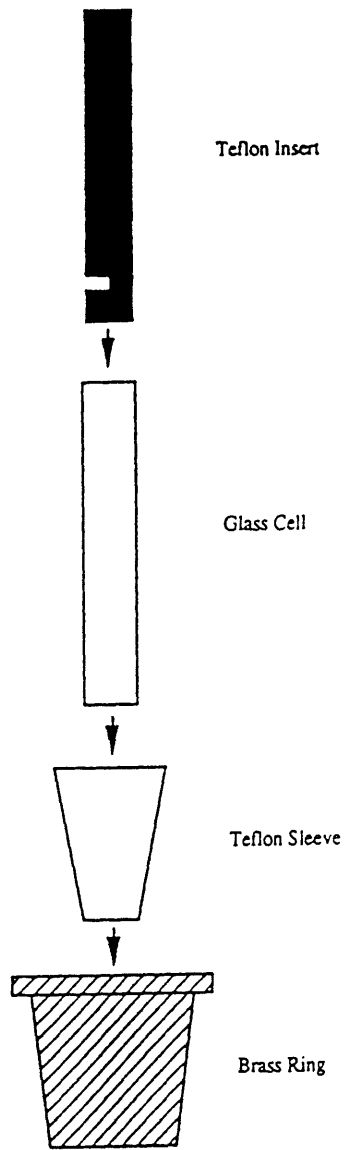


Figure 3-1: BI-SVC Sample Cell Schematic.

μl of filtered sample was injected into the tube, and the covered tube was positioned in the teflon sleeve/brass holder such that the laser beam passed through the sample below the meniscus.

Data Analysis. The time-dependent fluctuations in scattered light intensity detected by the electron tube can be represented by the second-order intensity autocorrelation function:

$$G^{(2)}(\tau) = \langle I(t)I(t+\tau) \rangle = \lim_{T \rightarrow \infty} \frac{1}{T} \int_0^T I(t)I(t+\tau)dt \quad (3.4)$$

where $G^{(2)}(\tau)$ denotes the time-averaged intensity, I , of the scattered light as a function of delay time, τ (the intensity will in general have different values at times t and $t+\tau$), and T represents the total duration of the experiment. This equation is written in terms of a continuous analog signal; in practice, the function is approximated by taking measurements over discrete intervals. The intensity is estimated by the number of photons n_i counted by the electron tube during a sampling interval $\Delta\tau$. In these terms Equation 3.4 is written as

$$G^{(2)}(\tau) = \langle n(t)n(t+\tau) \rangle = \lim_{N \rightarrow \infty} \sum_{i=1}^N n_i n_{i+j} \quad (3.5)$$

In this discrete version of Equation 3.4, $\tau = j\Delta\tau$, j takes on integer values from 1 to m where m is the number of channels in the autocorrelator, $t = i\Delta\tau$, and N is the total number of samples.

Division of Equation 3.5 by its baseline value ($G^{(2)}(\infty)$) gives the normalized second-order autocorrelation function

$$g^{(2)}(\tau) = \frac{G^{(2)}(\tau)}{G^{(2)}(\infty)} = \frac{\langle n(t)n(t+\tau) \rangle}{\langle n \rangle^2} \quad (3.6)$$

where $G^{(2)}(\infty)$ equals the square of the average photon counting rate, $\langle n \rangle^2$.

For a dilute solution of independently scattering molecules, the normalized second-

order autocorrelation function can be written as follows:

$$g^{(2)}(\tau) = 1 + \beta |g^{(1)}(\tau)|^2 \quad (3.7)$$

In Equation 3.7 β is an experimental variable related to the optical efficiency of the system, and $g^1(\tau)$ is the normalized first-order electric field autocorrelation function. For a monodisperse solution of rigid, spherical, optically isotropic particles, $g^1(\tau)$ can be described by the following exponential decay:

$$|g^{(1)}(\tau)| = \exp(-\Gamma\tau) \quad (3.8)$$

Here, Γ is the inverse time constant for the decay, and is described by

$$\Gamma = q^2 D \quad (3.9)$$

as $q \rightarrow 0$. In Equation 3.9, D is the translational diffusion coefficient, and q is the magnitude of the scattering vector:

$$q = \frac{4\pi n}{\lambda_0} \sin(\theta/2) \quad (3.10)$$

where n is the refractive index of the solvent, λ_0 is the wavelength of laser light *in vacuo*, and θ is the angle at which the scattered light is detected. In our studies, n was assumed to be equal to 1.33, λ_0 was equal to 514 nm, and θ was equal to 90°; therefore, $q = 0.023 \text{ nm}^{-1}$.

Equation 3.8 assumes a solution of monodisperse scatterers. For polydisperse systems, such as ours, Equation 3.8 must be rewritten:

$$|g^{(1)}(\tau)| = \sum_{m=1}^M G_m \exp(-\Gamma_m \tau) \quad (3.11)$$

where now $\Gamma_m = q^2 D_m$, D_m denoting the diffusion coefficient of the m th species, and G_m the normalized weighting factor which is proportional to the intensity of

light scattered by the m th species. Assuming a continuous distribution of scatterers, Equation 3.11 can be converted to integral form:

$$|g^{(1)}(\tau)| = \int_0^\infty G(\Gamma) \exp(-\Gamma\tau) d\Gamma \quad (3.12)$$

with

$$\int_0^\infty G(\Gamma) d\Gamma = \sum_{m=1}^? G_m = 1 \quad (3.13)$$

where $G(\Gamma)$ is in effect the distribution of diffusion coefficients, D .

Information regarding $G(\Gamma)$ can be obtained by the method of cumulants [24], which is based on exact correspondence between the form of Equation 3.12 and the moment generating function:

$$\ln|g^{(1)}(\tau)| = \frac{(-\tau)^n}{n!} k_n(\Gamma) \quad (3.14)$$

The cumulants k_n can be expressed in terms of the moments of the distribution; the experimental data are fit to the following equation:

$$\ln|\beta^{1/2}g^{(1)}(\tau)| = \ln\beta^{1/2} - \Gamma_z\tau + \frac{\mu_2\tau^2}{2} - \frac{\mu_3\tau^3}{6} \quad (3.15)$$

Only Γ_z and μ_2 can be determined with reasonable precision by this method [24].

It can be shown [4] that $\Gamma_z = q^2 D_z$, where D_z , the z -averaged diffusion coefficient, is defined by

$$D_z = \frac{\sum_m C_m M_m^2 P_m D_m}{\sum_m C_m M_m^2 P_m} \quad (3.16)$$

D_z can then be used in combination with the Stokes-Einstein equation to determine a z -averaged hydrodynamic radius:

$$D_z = \frac{kT}{6\pi\eta\langle R_h \rangle_z} \quad (3.17)$$

where k is Boltzmann's constant, T is the absolute temperature, and η is the viscosity of the solvent. Thus, a measure of the z -averaged size (in terms of a hydrodynamic radius) of the sample can be determined by this method of analysis.

Information regarding $G(\Gamma)$ can also be obtained by a data-fitting method known as constrained regularization [34]. Using this technique, an entire distribution of $G(\Gamma)$, as opposed to merely an average of the distribution, can be determined from the experimental data, $|g^{(1)}(\tau)|$. This is done by recognizing Equation 3.17 as having the form of a Fredholm integral of the first kind:

$$y(t) = \int_a^b F(\lambda, t)s(\lambda)d\lambda + \sum_{i=1}^{N_L} L_i\beta_i + \varepsilon \quad (3.18)$$

where $y(t)$ represent the noisy experimental data with experimental error ε , $F(\lambda, t)$ is some known function, and $s(\lambda)$ is the unknown function which is desired ($G(\Gamma)$ in this case). In the general case, L_i and β_i account for any constant terms present in the experiment; in our case, we attribute the β_i term to dust and set both N_L and L_i equal to one.

The problem of determining the function $s(\lambda)$ is in general an ill-posed one, as there may be many different solutions which are equally acceptable within the experimental error. The computer program CONTIN [35] solves this problem by first converting Equation 3.18 into a system of linear equations:

$$y(t) = \sum_{m=1}^{N_g} c_m F(\lambda_m, t)s(\lambda_m) + \sum_{i=1}^{N_L} L_i\beta_i + \varepsilon \quad (3.19)$$

where c_m are the weights of Simpson's formula and N_g are the grid points at which the solution is determined. Equation 3.19 can be rewritten in the following form:

$$y(t) = \sum_{j=1}^{N_x} A_{tj}x_j + \varepsilon \quad (3.20)$$

where $N_x = N_g + N_L$, \mathbf{A} is the matrix containing $c_m F(\lambda_m, t)$, and \mathbf{x} is a vector containing the unknowns $s(\lambda_m)$ and β_i . CONTIN then solves the system of equations under two constraints: $s(\lambda_m)$ must be non-negative, and parsimony or smoothness is imposed. This second constraint is met by adding a regularizing term to the normal least-squares minimization problem:

$$V(\alpha) = |\mathbf{M}_\epsilon^{-1/2}(\mathbf{y} - \mathbf{Ax})|^2 + \alpha^2 \int_a^b \left[\frac{d^2 s(\lambda)}{d\lambda^2} \right] d\lambda = \text{minimum} \quad (3.21)$$

Here, \mathbf{M}_ϵ is the covariance matrix of errors, ϵ , \mathbf{y} is the vector containing the data points $y(t)$, and α is a regularization parameter chosen by CONTIN such that the increase in $V(\alpha)$ over $V(\alpha = 0)$ will be due to chance alone approximately half of the time.

3.3 Results and Discussion

BSA Binding Experiments

Approximately 600 μg BSA was labelled with I^{125} using Pierce IODOBEAD reagent. Greater than 97% of the activity was precipitated by addition of 10% TCA. Specific activities between 1.6×10^{15} and 3.1×10^{16} CPM/mole ($\sim 0.01 - 0.21 \mu\text{Ci}/\mu\text{g}$ BSA) were measured.

Prior to the actual binding experiments, control experiments without mAb were performed to determine the amount of BSA- I^{125} adsorbing non-specifically to the anti-IgG-agarose beads. At BSA- I^{125} concentrations ranging from 3×10^{-9} – 3×10^{-7} M, less than 1% of the activity was contained in the precipitate, indicating that non-specific adsorption was negligible.

Radiolabelled BSA binding experiments were performed for each of the four mAb purified by affinity chromatography. Figures 3-2 through 3-5 contain binding isotherms and Scatchard plots obtained for each. The binding isotherms for mAb 3C2, 1N3 and 1N16 show the expected behavior, with the concentration of bound BSA increasing asymptotically toward a saturation value as the amount of BSA free in solution increases. The amount of BSA bound to mAb 3C9 also increases as the concentration of BSA in solution increases, as seen in Figure 3-3; however, the increase appears nearly linear, with no apparent leveling off in the isotherm. The saturation of this mAb appears to occur at concentrations of BSA higher than those used in these experiments.

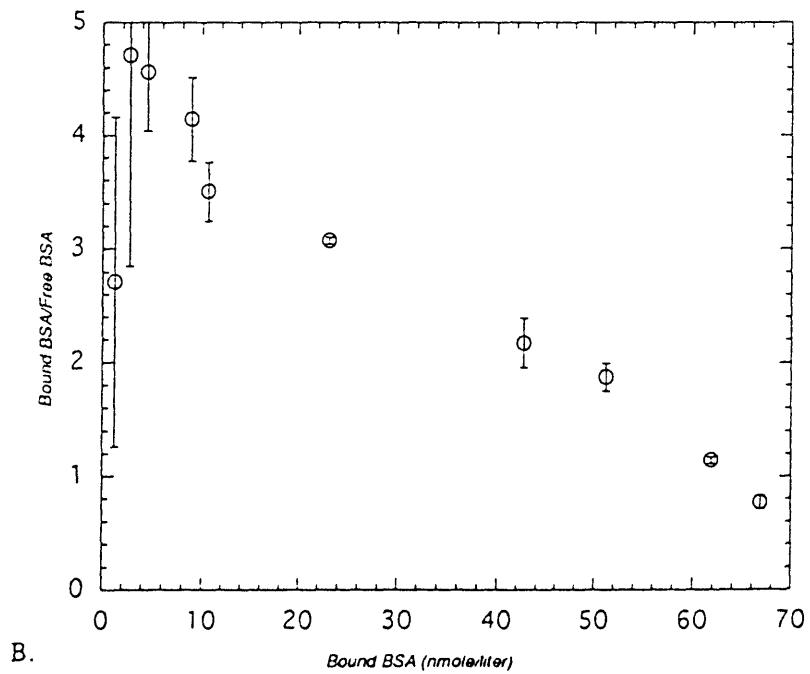
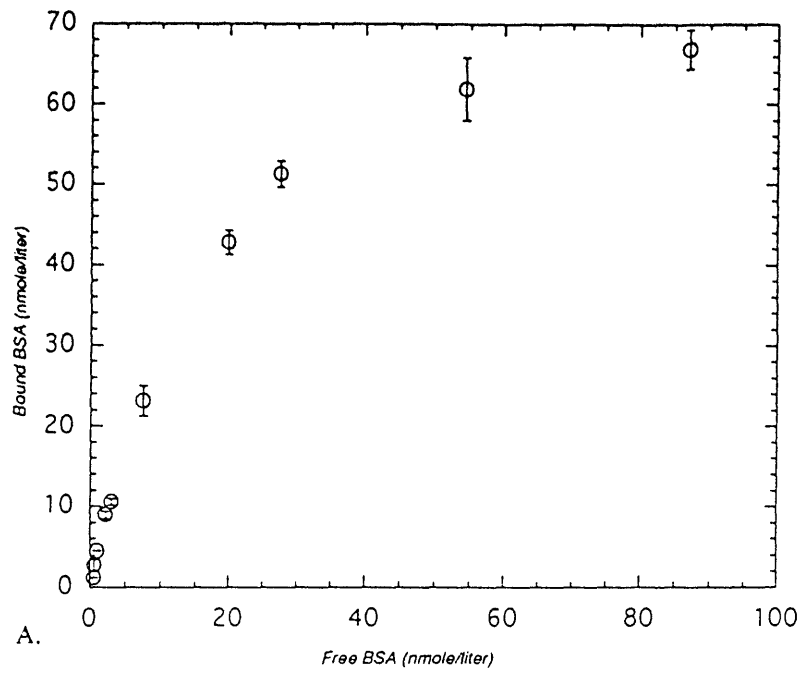


Figure 3-2: Binding Isotherm and Scatchard Plot for mAb 3C2. A. *Binding Isotherm*. B. *Scatchard Plot*. In both figures, data represent average \pm standard deviation of triplicate measurements.

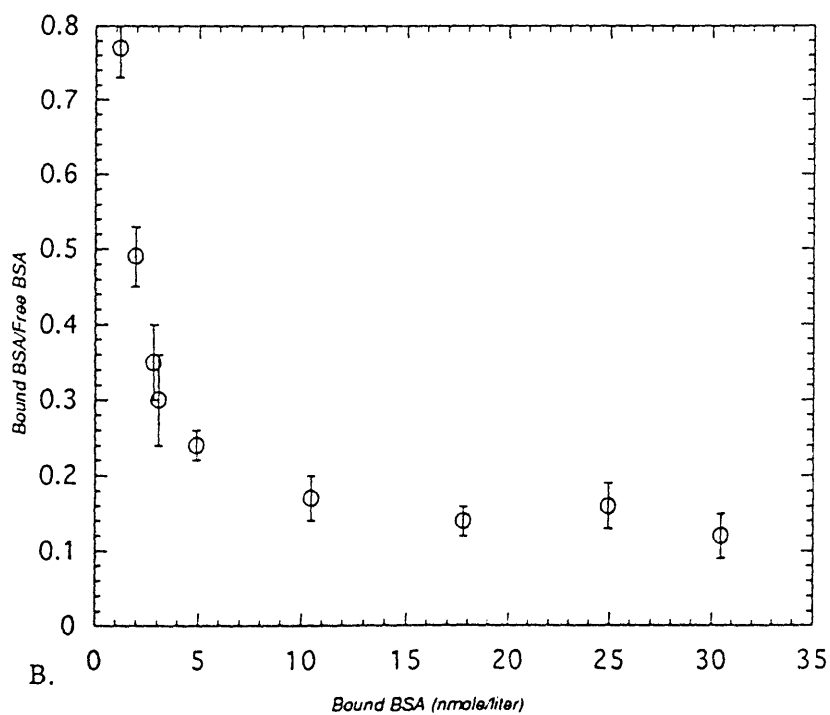
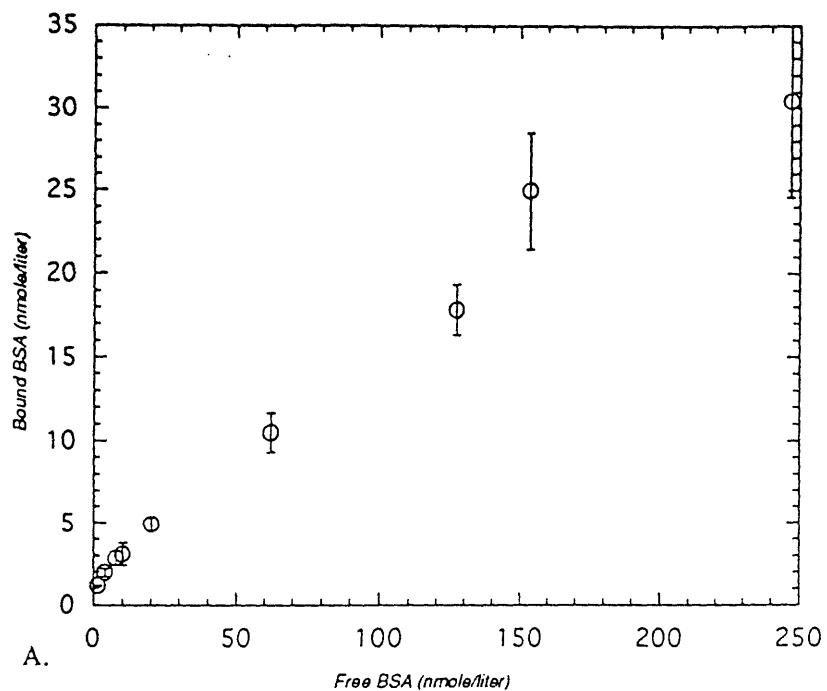


Figure 3-3: Binding Isotherm and Scatchard Plot for mAb 3C9. A. *Binding Isotherm.* B. *Scatchard Plot.* In both figures, data represent average \pm standard deviation of triplicate measurements.

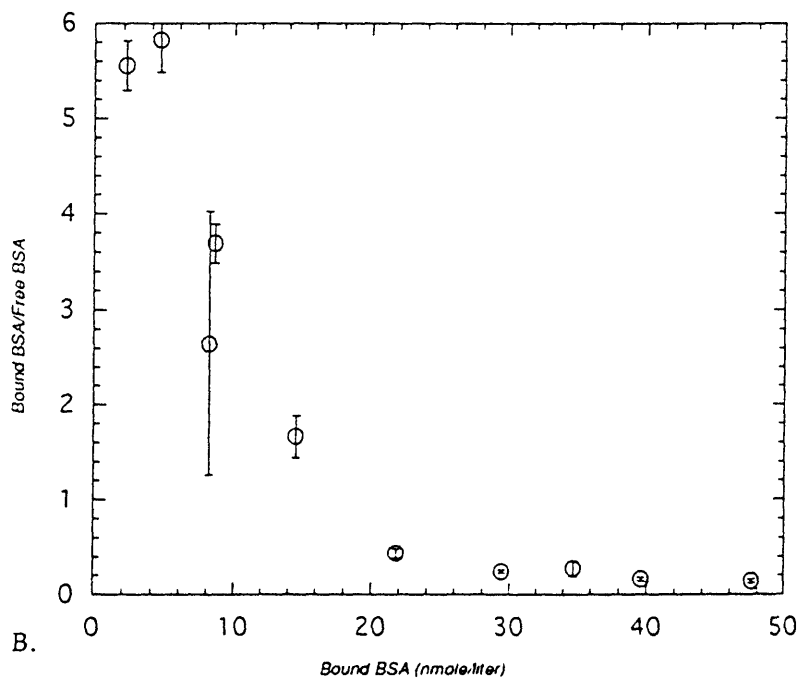
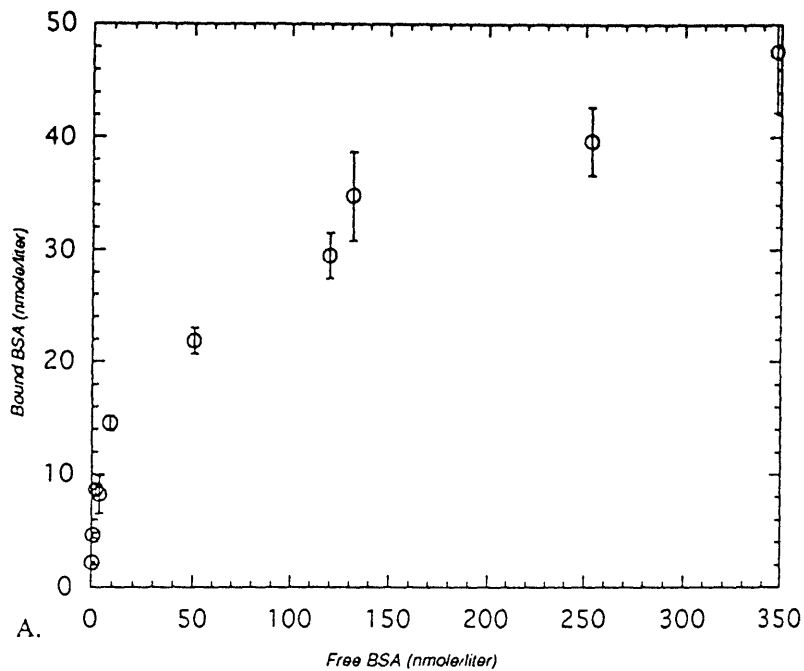


Figure 3-4: Binding Isotherm and Scatchard Plot for mAb 1N3. A. *Binding Isotherm.* B. *Scatchard Plot.* In both figures, data represent average \pm standard deviation of triplicate measurements.

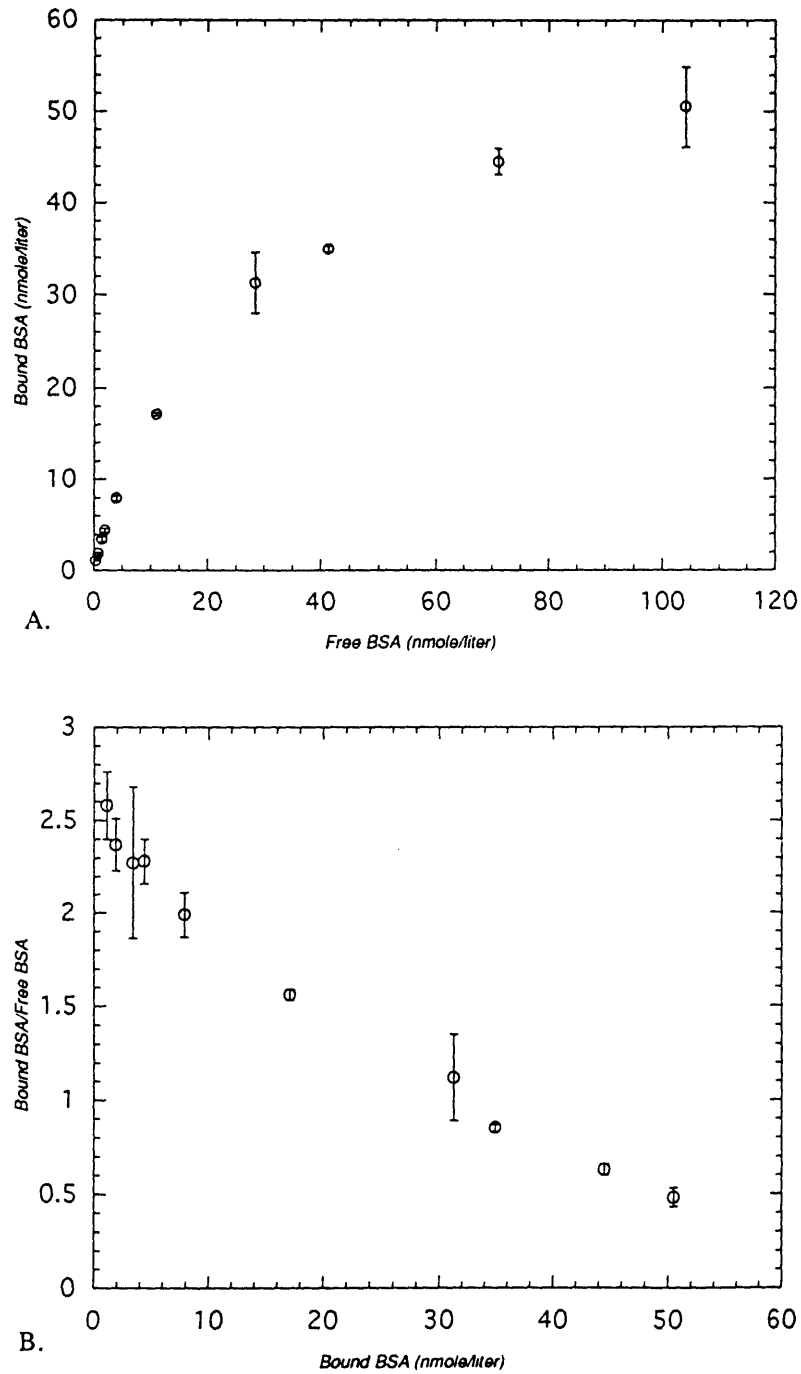


Figure 3-5: Binding Isotherm and Scatchard Plot for mAb 1N16. A. *Binding Isotherm*. B. *Scatchard Plot*. In both figures, data represent average \pm standard deviation of triplicate measurements.

mAb	K_a ($M^{-1} \times 10^{-8}$)	Correlation Coefficient, r
3C2	0.56 ± 0.06	-0.99
3C9	0.13	-0.69
1N3	1.2	-0.86
1N16	0.41 ± 0.04	-0.99

Table 3.1: mAb Association Constants.

The Scatchard plots contained in Figures 3-2 through 3-5 are plots of the ratio of bound to free BSA versus bound BSA concentration for each mAb studied. In general, they exhibit two types of behavior: those for mAb 3C2 and 1N16 show a fairly linear decrease of this ratio with increasing bound concentration, whereas those for 3C9 and 1N3 show a decrease with significant curvature. This would suggest that mAb 3C2 and 1N16 behave ideally in terms of their association with BSA; that is, they appear to bind non-cooperatively to a single epitope on the BSA molecule. 3C9 and 1N3, on the other hand, do not follow this behavior, and appear to bind the second BSA molecule with different affinity than the first, perhaps due to cross-reactions with other epitopes within the BSA structure.

Association constants were determined for each mAb from the Scatchard plot data. The data from each plot were fit by linear regression to Equation 3.3, and the resulting value for the slope was taken to be the association constant, K_a . In the case of mAb 3C2 and 1N16, the constant can be considered the intrinsic affinity constant, whereas for 3C9 and 1N3, it must be considered an average constant, due to the non-linear nature of the Scatchard data. The resulting values for each mAb, along with the linear correlation coefficients, are listed in Table 3.1. Experimental errors in the calculation of affinity constants were not determined for 3C9 and 1N3, due to the poor linear fit for these mAb.

The amount of BSA bound at saturation can be determined for each mAb from the x-intercept of the Scatchard plots. The corresponding values are: 3C2, 8.1×10^{-8} M; 3C9, 3.4×10^{-8} M; 1N3, 3.8×10^{-8} M; and 1N16, 5.9×10^{-8} M. We would expect a uniform value of 4×10^{-8} M for each of these mAb, since the concentration of mAb used for each assay was 2×10^{-8} M and at saturation there should be two molecules of BSA bound per mAb. The reason for this discrepancy is likely due to a systematic error

in measurement of mAb concentration. Concentrations of three mAb (3C2, 3C9 and 1N16) were determined by optical density measurements using an extremely small volume (50 μ l) spectrophotometer cell. It was later found that the optical density measurement obtained using this cell was highly dependent upon slight adjustments in the positioning of the cell within the spectrophotometer. Later measurements (for mAb 1N3) were obtained using a larger cell (500 μ l) which did not exhibit this systematic error. The saturation value obtained with this mAb is very near the expected value of 4×10^{-8} M.

QLS Experiments

IC were constructed in solution by mixing mAb 3C2 and 1N16 with BSA at a mAb₁:mAb₂:BSA molar ratio of 0.5:0.5:1.0, and the average size of the IC which were formed was measured using QLS and the method of cumulant analysis. To examine the dependence of this average size on the concentrations of the species involved, the BSA concentration was varied between 2×10^{-7} and 6×10^{-6} M. Figure 3-6 shows the results of the size measurements in terms of the average hydrodynamic radius, $\langle R_h \rangle_z$.

The plot shows an increase in $\langle R_h \rangle_z$ with increasing BSA concentration for this set of mAb. An increase of approximately 20% in $\langle R_h \rangle_z$ is observed over an approximate one and a half order of magnitude increase in BSA concentration. This is comparable to, although slightly less than, results observed with other sets of mAb pairs to BSA (between 33 and 70% increases in $\langle R_h \rangle_z$ over a nearly two order of magnitude increase in BSA concentration [44]). In contrast to those previous results, where the shape of the curve showed continuous growth with increasing BSA concentration, the data in Figure 3-6 show an apparent asymptotic growth toward some maximum size. Certainly, the expectation is for the size to continue to grow as concentrations are increased, with very large and insoluble aggregates ultimately being formed. The appearance of this maximum in Figure 3-6 may be due to the limited amount of data, however, and may not represent the true trend for this system.

CONTIN analysis of IC formed from BSA and three different pairs of mAb (3C2

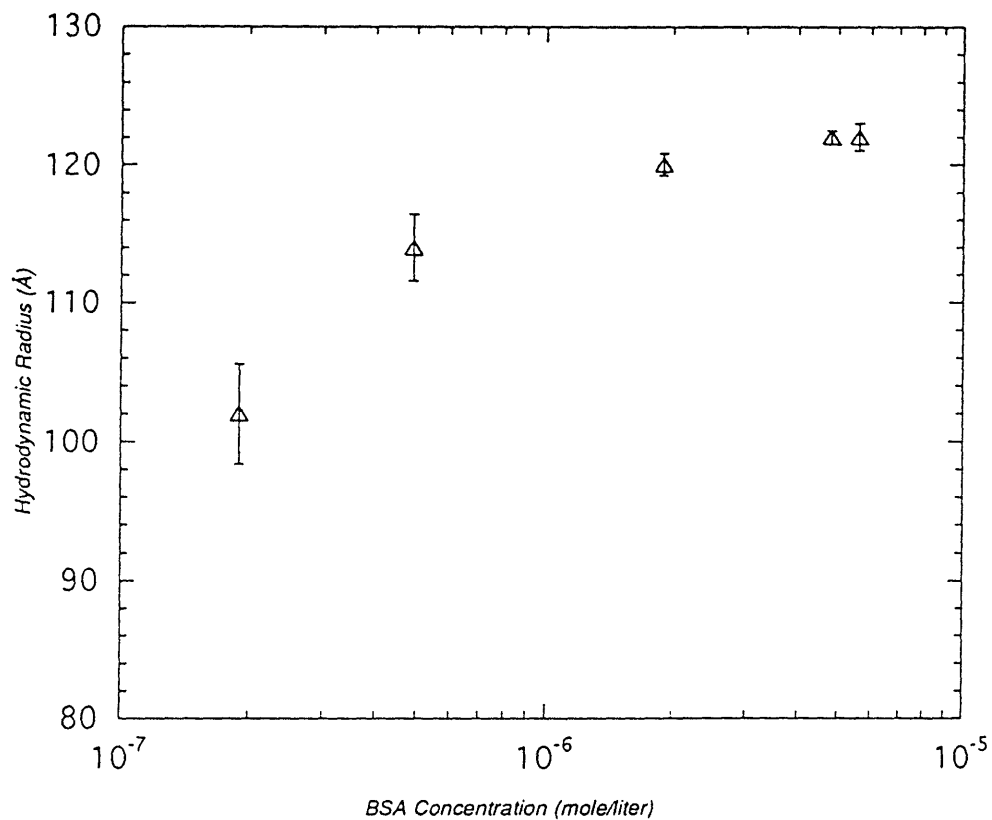


Figure 3-6: Effect of BSA Concentration on IC Size. *Equivalent hydrodynamic radius ($\langle R_h \rangle_z$) versus BSA concentration for IC constructed using mAb 3C2 and 1N16. Data points represent averages (\pm standard deviation) of triplicate measurements on a single sample.*

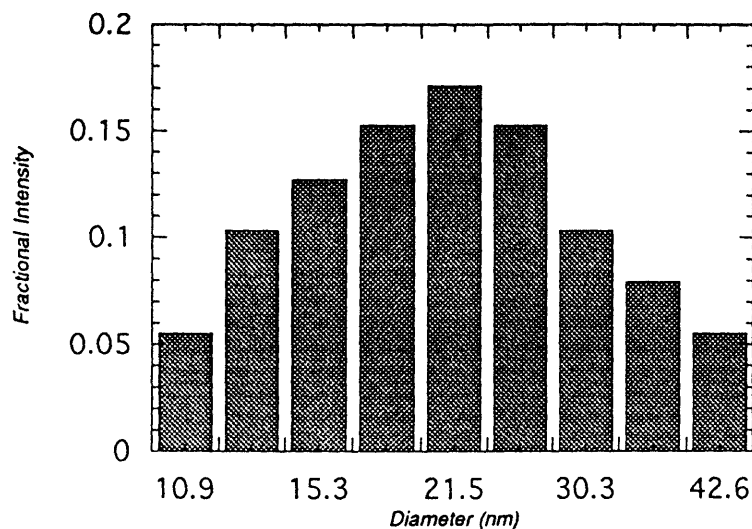


Figure 3-7: CONTIN Distribution. *Fractional intensity versus size for complexes prepared from BSA and mAb 3C2 and 1N16.*

+ 1N16, 3C2 + 1N3, and 3C9 + 1N16) was also performed to examine the size distribution of the IC being formed. IC were prepared at a single BSA concentration of 1×10^{-6} M and a $mAb_1:mAb_2:BSA$ molar ratio of 0.5:0.5:1.0. The resulting distributions are presented in Figures 3-7 through 3-9. Each of these figures represents a single measurement performed on a single sample.

In each case, the distributions fit to the data show the presence of species with diameters ranging between 6 and 50 nm (60 to 500 Å). The means of the three distributions are 22, 22, and 21 nm for 3C2 + 1N16, 3C2 + 1N3, and 3C9 + 1N16, respectively. If the diffusion coefficient of an IgG molecule in solution is taken to be 3.9×10^{-7} $\text{cm}^2 \text{sec}^{-1}$ [37], resulting in a Stokes diameter of 10.8 nm, these distributions would suggest that IC composed of up to four or five mAb are being formed, with the mean size representing complexes containing two mAb.

A few subtle differences can be seen among the three distributions in Figures 3-7 through 3-9. The distributions in Figures 3-7 and 3-9 both appear reasonably symmetric; however, the overall distribution in Figure 3-9 is shifted toward a lower Stokes diameter than that in Figure 3-7. It is also interesting to note the presence

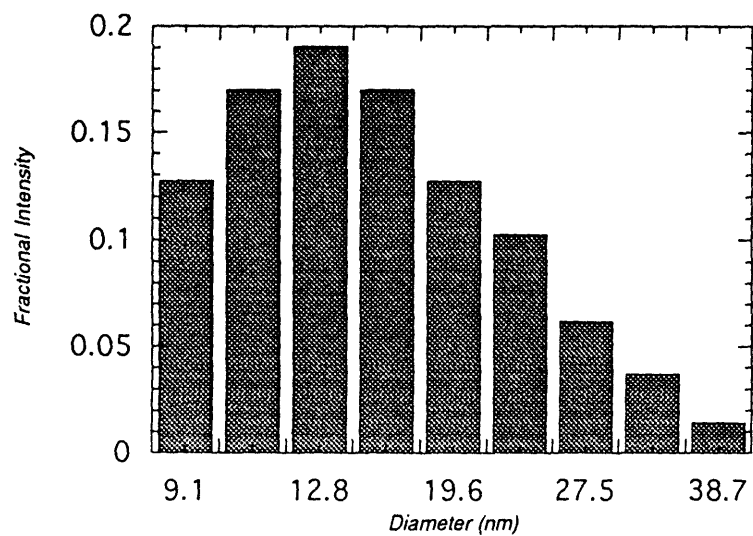


Figure 3-8: CONTIN Distribution *Fractional intensity versus size for complexes prepared from BSA and mAb 3C2 and 1N3.*

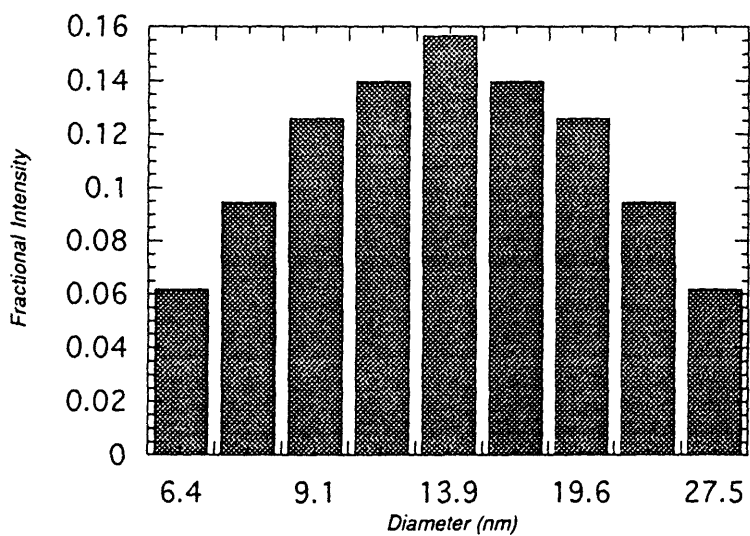


Figure 3-9: CONTIN Distribution. *Fractional intensity versus size for complexes prepared from BSA and mAb 3C9 and 1N3.*

of species of approximately 6.5 nm in the distribution for 3C9 + 1N16. A value for the hydrodynamic radius of BSA measured by QLS has previously been reported to be 3.6 nm (7.2 nm in diameter) [44]; thus, the presence of this small species in the distribution for this pair of mAb would suggest that a large fraction of the BSA remained unbound at this concentration. Finally, in slight contrast to the other two, the distribution in Figure 3-8 appears non-symmetric, and displays a higher fraction of smaller species relative to larger species within the distribution.

Although differences in the distributions can be seen, none appears to be exceptionally dramatic, suggesting little differences among the IC that are formed by these three sets of mAb pairs. This may be due to the fact that within each pair, one of the mAb involved bound to the 3C subdomain of BSA, and the other bound to the 1N region. Previous work in our laboratory has shown that both the average size of IC and their propensity to form cycles may be more strongly influenced by the spatial locations of the antigenic epitopes than by the intrinsic affinities of the mAb involved [43, 30]. In the case of IC involving mAb 1N3 and 3C9, we might expect larger aggregates to form if indeed these mAb were cross-reactive with other epitopes. Again, however, the location and nature of such cross-reactive epitopes might preclude such multivalent binding from occurring. Regardless of these issues, the results of this study suggest that mixtures of these pairs of mAb and BSA consist of multimeric IC large enough for use in complement binding and activation experiments [12].

Chapter 4

Conclusions and

Recommendations for Future

Work

In this thesis, monoclonal antibodies to bovine serum albumin were purified from mouse ascites fluid by use of two different affinity chromatography media: Sepharose CL-4B and an Acti-Disk GTA cartridge, both of which containing immobilized BSA as the affinity ligand. For Sepharose, CDAP activation chemistry was utilized for ligand attachment; for the Acti-Disk, the ligand was coupled via pre-existing glutaraldehyde groups according to the manufacturer's protocol. Both methods resulted in reasonable quantitative attachment of BSA, with a five milliliter column of the Sepharose and the Acti-Disk cartridge containing 17.5 and 19.4 mg, respectively. The inability to achieve the maximum theoretical capacity with both materials was most likely due to diffusional limitations in the case of Sepharose, and to improper flow distribution in the case of the Acti-Disk.

These affinity materials were used to successfully purify four out of a panel of five monoclonal antibodies to BSA in significant quantities. Three slightly different methods were performed: the Sepharose column was used with application of a low pH glycine buffer to elute the bound antibody, and the Acti-Disk cartridge was used both with and without an extra washing step to enhance purity prior to low pH

elution. The average yields for the four clones purified (3C2, 3C9, 1N3, and 1N16) were between 2 and 6 mg/ml of loaded ascites fluid, suggesting concentrations in ascites which are typical for monoclonal antibodies raised in mouse. Attempts to purify the fifth monoclonal (2-11) were unsuccessful, suggesting either an extremely low affinity of this antibody for BSA, or a significantly lower titre of the antibody in the ascites fluid received.

Native PAGE gels of the protein obtained using each of the three methods showed a significant difference in product homogeneity among the methods used. The protein obtained using the Acti-Disk cartridge without the extra washing step appeared to consist of a large number of proteins of varying molecular weight. This poor separation was deemed unsatisfactory, and prompted the inclusion of the extra step when using that device. Addition of the high salt wash resulted in a vast improvement in antibody purity, and yielded a product which could be used in further experiments with only minor additional treatment. Finally, the protein obtained using the Sepharose column displayed the greatest homogeneity of all three, with only a single band corresponding to monoclonal antibody appearing on the gel.

Association constants were determined for each of the four monoclonals purified using radioiodinated BSA in a radioimmunoassay. Association constants were determined from Scatchard plots of the data and followed the trend $1N3 > 3C2 > 1N16 > 3C9$. The data conformed well to a linear relationship for clones 3C2 and 1N16; thus, the affinity constants determined for these antibodies can be regarded as intrinsic binding constants. The data for clones 3C9 and 1N3 did not exhibit linear behavior, suggesting possible cooperativity effects and cross-reaction, and can therefore only be regarded as average binding constants.

Quasi-elastic light scattering performed on mixtures of pairs of antibodies and BSA demonstrated that complexes of antigen and antibody were being formed in these mixtures. In the case of one set (3C2 + 1N16), the average hydrodynamic size of the system increased with increasing concentration of reactants, indicating that the increased concentration was shifting the equilibrium toward larger and larger complexes. Size distributions were also obtained for this set and two other sets (3C2

+ 1N3, and 3C9 + 1N16) by CONTIN fit of the experimental data. The results indicated that distributions of aggregates composed of between one and four to five antibodies were being formed at the concentration studied.

Future work in this area could be extended in a number of directions. First, the primary motivation for the work reported here was to obtain and characterize monoclonal antibodies suitable for use in complement binding and activation studies. The logical extension would be to use these antibodies to construct immune complexes for that purpose, beginning with an investigation of their binding to the first component of the cascade, C1q, and continuing with experiments involving other relevant complement proteins.

Second, electron microscopy could be utilized in order to visualize the complexes which are formed, both in the presence and absence of complement proteins. Micrographs obtained could be used to verify results from light scattering, and in the case where complement proteins are included, could be analyzed to gain new insight into the complex-complement association and the effects of this association on complex size.

Third, complexes formed with these antibodies could be used to further study the equilibrium and kinetics of their association with a number of Fc-binding proteins, most notably the immunoadsorbent molecule *Staphylococcal* protein A. The inclusion of complement components in these experiments would allow a quantitative measure of the competition between all these proteins for closely-situated binding sites on the antibody molecule.

Finally, future research could focus on increasing the complexity of the system by studying complexes formed from three and possibly more monoclonal antibodies. Such a system should more accurately represent the *in vivo* case of polyclonal antibody, but would require additional antibodies (associating with a different BSA subdomain) than those characterized in this thesis.

Bibliography

- [1] R. W. Baldwin and R. A. Robbins. Circulating immune complexes in cancer. In S. Sell, editor, *Cancer Markers: Diagnostic and Developmental Significance*, chapter 19, pages 507–531. Humana Press, Clifton, New Jersey, 1980.
- [2] D. C. Benjamin and J. M. Teale. The antigenic structure of bovine serum albumin: Evidence for multiple, different, domain-specific antigenic determinants. *Journal of Biological Chemistry*, 253:8087–8092, 1978.
- [3] V. A. Bloomfield and T. K. Lim. Quasi-elastic laser light scattering. *Methods in Enzymology*, pages 415–495, 1978.
- [4] J. C. Brown, P. N. Pusey, and R. Dietz. Photon correlation study of polydisperse samples of polystyrene in cyclohexane. *Journal of Chemical Physics*, 62:1136–1144, 1975.
- [5] J. R. Brown. Structural origins of mammalian albumin. *Federation Proceedings*, 35:2141–2144, 1976.
- [6] D. R. Burton and J. M. Woof. Human antibody effector function. In Frank J. Dixon, editor, *Advances in Immunology*, number 51, pages 1–84. Academic Press, Inc., 1992.
- [7] D. H. Campbell, E. Luescher, and L. S. Lerman. Immunologic adsorbents. I. Isolation of antibody by means of a cellulose-protein antigen. *Proceedings of the National Academy of Science*, 37:575–578, 1951.

- [8] C. Carini, I. Mezzaroma, G. Scano, R. D'Amelio, P. Matricardi, and F. Aiuti. Characterization of specific immune complexes in hiv-related disorders. *Scandinavian Journal of Immunology*, 26:21–28, 1987.
- [9] S. J. Chester, P. Maimonis, P. A. Meitner, and M. P. Vezeridis. An analysis of immunocomplexes for the detection of the early stages of colon cancer. *Cancer*, 65:1338–1344, 1990.
- [10] B. J. Davis. Disc electrophoresis II: Methods and application to human serum proteins. *Annals of the New York Academy of Science*, 121:404–427, 1964.
- [11] R. O. Dillman. Monoclonal antibodies for treating cancer. *Annals of Internal Medicine*, 111:592–603, 1989.
- [12] G. Doekes, L. A. van Es, and M. R. Daha. Binding and activation of the first complement component by soluble immune complexes: Effect of complex size and composition. *Scandinavian Journal of Immunology*, 19:99–110, 1984.
- [13] H. N. Eisen. *General Immunology*. J. B. Lippencott Co., Philadelphia, 1990.
- [14] L. R. Espinoza. Assays for circulating immune complexes. In *Circulating Immune Complexes: Their Clinical Significance*, chapter 3, pages 63–86. Academic Press, 1983.
- [15] P. L. Ey, S. J. Prowse, and C. R. Jenkin. Isolation of pure IgG₁, IgG_{2a}, and IgG_{2b} using protein A-sepharose. *Biochemistry*, 15:429–436, 1978.
- [16] J. W. Goding. *Monoclonal Antibodies: Principles and Practice*, chapter 6, pages 219–240. Academic Press, Inc., second edition, 1986.
- [17] R. Gross, M. L. Yarmush, J. W. Kennedy, and L. V. Quintas. Antigenesis: A cascade-theoretical analysis of the size distributions of antigen-antibody complexes. *Discrete Applied Mathematics*, 19:177–194, 1988.
- [18] A. E. Gurvich and Drizlikh G. I. Use of antibodies on an insoluble support for specific detection of radioactive antigens. *Nature*, 5:648–649, 1964.

- [19] P. J. Hogg, S. C. Johnston, M. R. Bowles, S. M. Pond, and D. J. Winzor. Evaluation of equilibrium constants for antigen–antibody interactions by solid-phase immunoassay: The binding of paraquat to its elicited mouse monoclonal antibody. *Molecular Immunology*, 24:797–801, 1987.
- [20] V. Holmskov-Nielsen, J. C. Jensenius, K. Erb, and S. Husby. Immune complex formation analyzed by high-performance size exclusion chromatography using either I¹²⁵-labelled antigen or enzyme-linked immunosorbent assay for detection. *Immunology*, 51:809–814, 1984.
- [21] G. Köhler and C. Milstein. Continuous cultures of fused cells secreting antibody of predefined specificity. *Nature*, 256:495–497, 1975.
- [22] J. Kohn and M. Wilchek. 1-Cyano-4-dimethylamino pyridinium tetrafluoroborate as a cyanalating agent for the covalent attachment of ligand to polysaccharide resins. *FEBS Letters*, 154:209–211, 1983.
- [23] J. Kohn and M. Wilchek. The use of cyanogen bromide and other novel cyanalating agents for the activation of polysaccharide resins. *Applied Biochemistry and Biotechnology*, 9:285–305, 1984.
- [24] D. E. Koppel. Analysis of macromolecular polydispersity in intensity correlation spectroscopy: The method of cumulants. *Journal of Chemical Physics*, 57:4814–4820, 1972.
- [25] Å. Larsson, R. Ghosh, and S. Hammarström. Determination of intrinsic affinity constants of monoclonal antibodies against carcinoembryonic antigen. *Molecular Immunology*, 24:569–576, 1987.
- [26] W. G. Laver and G. M. Air, editors. *Immune Recognition of Protein Antigens*. Cold Spring Harbor Laboratory, Cold Spring Harbor, New York, 1985.
- [27] M. Mannik. Physicochemical and functional relationships of immune complexes. *Journal of Investigative Dermatology*, 74:333–338, 1980.

- [28] G. A. Morel, D. M. Yarmush, C. K. Colton, D. C. Benjamin, and M. L. Yarmush. Monoclonal antibodies to bovine serum albumin: Affinity and specificity determinations. *Molecular Immunology*, 425:7–15, 1988.
- [29] R. M. Murphy, R. A. Chamberlin, P. Schurtenberger, C. K. Colton, and M. L. Yarmush. Size and structure of antigen-antibody complexes: Thermodynamic parameters. *Biochemistry*, 29:10889–10899, 1990.
- [30] R. M. Murphy, H. Slayter, P. Schurtenberger, R. A. Chamberlin, C. K. Colton, and M. L. Yarmush. Size and structure of antigen-antibody complexes: Electron microscopy and light scattering studies. *Biophysical Journal*, 54:45–56, 1988.
- [31] R. M. Murphy, M. L. Yarmush, and C. K. Colton. Determining molecular weight distributions of antigen-antibody complexes by quasi-elastic light scattering. *Biopolymers*, 31:1289–1295, 1991.
- [32] H. L. Niman and J. H. Elder. mAbs as probes of protein structure: Molecular diversity among the envelope glycoproteins (gp70s) of the murine retroviruses. In David H. Katz, editor, *Monoclonal Antibodies and T Cell Products*, chapter 2, pages 23–52. CRC Press, Inc., Boca Raton, Florida, 1982.
- [33] H. Nygren, M. Kaartinen, and M. Stenberg. Determination by ellipsometry of the affinity of monoclonal antibodies. *Journal of Immunological Methods*, 92:219–225, 1986.
- [34] S. W. Provencher. A constrained regularization method for inverting data represented by linear algebraic or integral equations. *Computational Physics Communications*, 27:213–227, 1982.
- [35] S. W. Provencher. CONTIN: A general purpose constrained regularization program for inverting noisy linear algebraic and integral equations. *Computational Physics Communications*, 27:229–242, 1982.

- [36] A. H. Ross, D. Herlyn, and H. Koprowski. Purification of monoclonal antibodies from ascites using ABx liquid chromatography column. *Journal of Immunological Methods*, 102:227–231, 1987.
- [37] H. A. Sober, editor. *Handbook of Biochemistry*. The Chemical Rubber Company, Cleveland, second edition, 1970.
- [38] H. L. Spiegelberg. Biological activities of immunoglobulins of different classes and subclasses. In Frank J. Dixon, editor, *Advances in Immunology*, number 19, pages 259–294. 1974.
- [39] J. Steensgard, C. Jacobsen, J. Lowe, N. R. Ling, and R. Jefferis. Theoretical and ultracentrifugal analysis of immune complex formation between monoclonal antibodies and human IgG. *Immunology*, 46:751–760, 1982.
- [40] A. K. Szakal, M. H. Kosco, J. P. Smith, and J. G. Tew. Use of monoclonal antibodies in immunocytochemistry and at the light and electron microscopic levels. In Lawrence B. Schook, editor, *Monoclonal Antibody Production Techniques and Applications*, pages 229–264. Marcel Dekker, Inc., 1987.
- [41] A. Theofilopoulos and F. J. Dixon. The biology and detection of immune complexes. In F. J. Dixon, editor, *Advances in Immunology*, number 28, chapter 3, pages 179–183. Academic Press, Inc., 1979.
- [42] J. W. Uhr, K. A. Krolick, and E. S. Vitetta. Selective killing of leukemia cells by antibody-toxin conjugates. In J. Thomas August, editor, *Monoclonal Antibodies in Drug Development*, pages 172–176. American Society for Pharmacology and Experimental Therapeutics, 1982.
- [43] D. M. Yarmush, G. Morel, and M. L. Yarmush. A new technique for mapping epitope specificities of monoclonal antibodies using quasi-elastic light scattering spectroscopy. *Journal of Biochemical and Biophysical Methods*, 14:279–289, 1987.

- [44] D. M. Yarmush, R. M. Murphy, C. K. Colton, M. Fisch, and M. L. Yarmush. Quasi-elastic light scattering of antigen-antibody complexes. *Molecular Immunology*, 25:17–32, 1988.
- [45] H. Zola and D. Brooks. Techniques for the production and characterization of monoclonal hybridoma antibodies. In J. G. R. Hurrell, editor, *Monoclonal Hybridoma Antibodies: Techniques and Applications*, chapter 1, pages 4–57. CRC Press, Inc., Boca Raton, Florida, 1982.